じて Bio-Gel P-2 (Bio-Rad) カラムで処理した部分精製毒を LC/MS 分析に供した．本分析は Hashimoto らの方法[28]に準拠し，MS 部に高速噴霧イオン化 (SSI) 法を備えた M-8000 (Hitachi) を用い，ポジティブモード，第一細孔温度 170℃，シールド温度 300℃，検出器電圧 400 V，フォーカス電圧 30 V，ドリフト電圧 30 V で行った．

結　　果

1. *A. tamiyavanichii* の細胞密度

2004 年 10 月 16 日の St. 1～5 における *A. tamiyavanichii* の細胞密度は 96～4,960 cells/L（平均細胞密度±標準偏差：1,554±1820 cells/L，以下同様）であったが，10 月 19 日には St. 1～4 で 0～16 cells/L (4.2±6.8 cells/L) と急激に減少した．その後，11 月 4 日に St. 6 で 350 cells/L が観測された (Table 1)．一方，*A. tamiyavanichii* 以外の既知の PSP 産生渦鞭毛藻は期間を通して全く観察されなかった．

2. *A. tamiyavanichii* とムラサキイガイの毒性

Table 1 に各試料の毒性を示す．*A. tamiyavanichii* 天然藻体については，供試 5 藻体中，十分な細胞数が得られた 2 藻体（At2 および At4）でのみマウス毒性を測定することができ，毒力はそれぞれ 15.4 および 6.25×10^{-4} MU/cell で，相互に大きな差異があった．一方，培養 4 藻体は $2.7\sim3.5\times10^{-4}$ MU/cell と，互いに類似した毒力を示した．他方，ムラサキイガイ（Mg4 および Mg2）は共に有毒で，毒力はそれぞれ 28 および 13 MU/g であった．

3. *A. tamiyavanichii* とムラサキイガイの毒成分

HPLC 分析における各試料のクロマトグラムを Fig. 2，それらから算出した成分ごとの物質量を Table 2 に示す．総 PSP 量は，供試した天然 2 藻体で 2,410 および 840 fmol/cell，培養 4 藻体で 220～359 fmol/cell と毒力同様，前者のほうが後者よりも高かった．天然藻体では GTX5 の含量が最も多く（1,260 および 341 fmol/cell），次いで GTX4, STX, PX2, GTX6, GTX3, GTX1 の順となった．少量の PX1, GTX2 および neoSTX も検出された．一方，培養藻体では GTX3, GTX5, PX2, GTX2, STX, neoSTX, および GTX4 の含量が比較的多く（それぞれ平均毒量 103, 51.6, 38.6, 21.8, 21.6, 14.2 および 12.2 fmol / cell），その他に少量の PX1, dcGTX3, GTX1, hySTX を含んでいた．すなわち，天然藻体は GTX5 (52.4 および 40.6 mol%) を主成分，GTX4 (15.6 および 24.8 mol%) や STX (15.8 および 13.8 mol%) を主な副成分とするのに対し，培養藻体は GTX3 (平均 37.6 mol%，以下同様) が主成分，GTX5 (18.1 mol%) や PX2 (12.8 mol%) が主要な副成分で，GTX4 はわずか 4.7 mol%, STX も 7.7 mol% しか含まれていなかった (Fig. 3)．

ムラサキイガイの試料のうち，毒力の高かった Mg4 につき，HPLC 分析に供したところ，総 PSP 量は 37.6 nmol/g と算出された (Fig. 2, Table 2)．主成分は GTX4 および GTX5 で，23.8 mol% (8.92 nmol/g) および 22.5 mol% (8.46 nmol/g) を占めており，副成分として STX や GTX1, GTX3 が含まれていた (Table 2, Fig. 3)．微量の PX1, 2, GTX2, GTX6, dcGTX2, neoSTX も検出された．

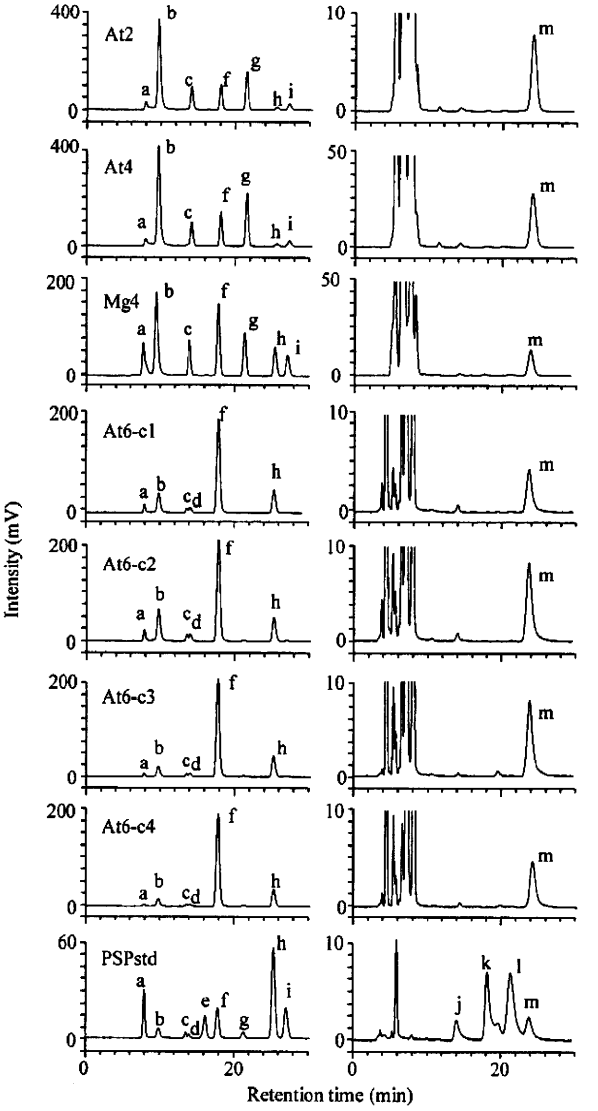

Fig. 2. HPLC chromatograms of extracts from *A. tamiyavanichii* and mussel *M. galloprovincialis*, and of PSP standards.

At2 and At4: wild cells of *A. tamiyavanichii*; At6-c1, At6-c2, At6-c3 and At6-c4: cultured cells of *A. tamiyavanichii*; Mg4: *M. galloprovincialis*. a: PX1 (C1); b: PX2 (C2); c: GTX5; d: dcGTX3; e: dcGTX2; f: GTX3; g: GTX4; h: GTX2; i: GTX1; j: neoSTX; k: hySTX; l: dcSTX; m: STX

既報[1]の比毒性に基づき各試料の PSP 量を毒力に換算したところ，天然藻体は 21.5 および 8.7×10^{-4} MU/cell，培養藻体は $2.8\sim3.8\times10^{-4}$ MU/cell，ムラサキイガイは 50 MU/g となった (Table 1)．

Mg4 の LC/MS 分析では，基本的に HPLC 分析と一致す

Table 2. Amount of each PSP component in wild and cultured cells of *A. tamiyavanichii*, and in mussel *M. galloprovincialis*

Component	*A. tamiyavanichii* (wild)		*A. tamiyavanichii* (cultured)					*M. galloprovincialis*
	At2	At4	At6-c1	At6-c2	At6-c3	At6-c4	Mean±SD	Mg4
	(fmol/cell)		(fmol/cell)					(nmol/g)
PX1 (C1)	10.4	5.94	11.1	16.9	5.09	3.12	9.05±5.40	1.27
PX2 (C2)	127	56.5	43.1	71.4	22.1	17.8	38.6±21.2	2.44
GTX1	63.6	25.9	2.55	2.60	4.80	2.17	3.03±1.03	4.80
GTX2	6.56	2.37	23.1	24.2	22.6	17.3	21.8±2.65	1.25
GTX3	58.5	31.2	96.2	109	109	100	103±5.48	3.64
GTX4	375	208	6.44	9.36	14.6	18.3	12.2±4.60	8.92
GTX5	1,260	341	68.2	63.8	39.9	34.6	51.6±14.6	8.46
GTX6	114	45.8	—	—	—	—	—	1.28
dcGTX2	—	—	—	—	—	—	—	0.0976
dcGTX3	—	—	6.41	9.29	4.77	3.06	5.88±2.30	—
neoSTX	9.61	6.36	19.2	24.2	7.14	6.08	14.2±7.76	0.207
hySTX	—	—	—	—	4.25	1.21	2.73	—
STX	381	116	12.5	27.7	30.2	15.8	21.6±7.55	5.17
Total	2,410	840	289	359	264	220	283±58.1	37.6

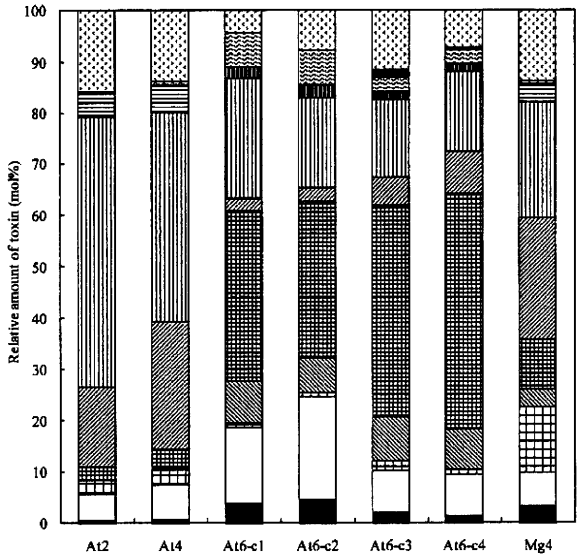

Fig. 3. Toxin composition of wild and cultured cells of *A. tamiyavanichii*, and of mussel *M. galloprovincialis*

■ PX1 (C1); □ PX2 (C2); ⊞ GTX1; ▨ GTX2; ▦ GTX3; ▨ GTX4; ▥ GTX5; ▤ GTX6; ▬ dcGTX2; ▥ dcGTX3; ▩ hyneoSTX; ▩ neoSTX; ▩ hySTX; ■ dcSTX; ⊡ STX

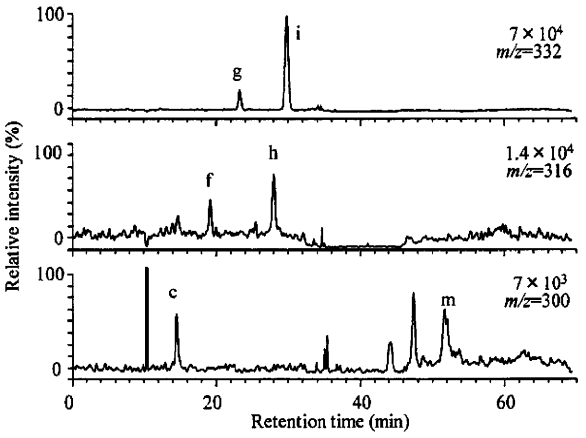

Fig. 4. Selected ion mass chromatograms (*m/z* 300, 316 and 332) of partially purified toxin from mussel *M. galloprovincialis* (Mg4).

る結果が得られた．すなわち，*m/z* 300 のクロマトグラムにおいて GTX5 ($[M+H-SO_3]^+=300$) と STX ($[M-H]^+=300$), *m/z* 316 で GTX3 ($[M-H-SO_3]=316$) と GTX2 ($[M+H-SO_3]^+=316$), *m/z* 332 で GTX4 ($[M+H-SO_3]^+=332$) と GTX1 ($[M+H-SO_3]^-=332$) が検出された (Fig. 4).

考　　察

本研究では，播磨灘の 6 地点で採水した海水中に最高 4,960 cells/L の密度で *A. tamiyavanichii* が観察された．同海域では，1999 年に最高 30,000 cells/L，その後も 2003 年にかけて最高 8,000～27,000 cells/L の密度で同種の出現が観測されている[10)～15)]．これらと比較して，今回の調査で確認された *A. tamiyavanichii* の出現密度は特に高いものではなかった．

一方，*A. tamiyavanichii* 天然藻体（At2 および At4）の毒力は，それぞれ 15.4 および 6.25×10^{-4} MU/cell と測定された．また，これらとほぼ同時期同海域で採取したムラサキイガイ（Mg2 および Mg4）の毒力は 13 および 28 MU/g であった．Hashimoto ら[9)]によれば，1999 年に播磨灘で発生した *A. tamiyavanichii* 天然藻体の毒力は 13.9×10^{-5} MU/cell，そのときのムラサキイガイの毒力は最高 7.3 MU/g であったという．すなわち，今回得た藻体の毒力は，Hashimoto らのものより 5～11 倍も高かったわけであり，ムラサキイガイが 28 MU/g と比較的高い水準にまで毒化したのは，*A. tamiyavanichii* の出現密度というよりは 1 細胞当たりの毒力が通常より高かったため

と推察される.

他方, *A. tamiyavanichii* 培養藻体 (At6-c1～c4) の毒力は, 2.7～3.5×10^{-4} MU/cell と天然藻体よりは低かったが, Beppu ら[6]が 2004 年に瀬戸内海備後灘から分離した *A. tamiyavanichii* 培養藻体の毒力と比較すると 2～9 倍も高かった. 培養藻体の毒力が天然藻体のそれより低いのは PSP 産生渦鞭毛藻では一般的な現象であり[29], At6 も, 本来, 高い毒産生能を有していたと推察される.

次に, 毒組成を見ると, 今回採取した *A. tamiyavanichii* 天然藻体は GTX5 を主成分とし, 加えて相当量の GTX4, STX などを含んでいた. これに対し, Hashimoto ら[9]の天然藻体は GTX4 を主成分, GTX2, 3 を主要な副成分としていた. すなわち, 著量の GTX4 を含む点では両者は一致したが, 本研究の藻体では GTX5, Hashimoto らの藻体では GTX2, 3 の割合が高いという点で大きく異なっていた. Lim ら[30]は, 本種を低い温度 (20℃) で培養すると, GTX4 の産生量が減少し, GTX3 量が増加すること, 照度が低いと温度が高くても GTX3 量が増加することを報告している. 藻体の採取月 (本研究では 10 月, Hashimoto らの場合は 12 月) を考慮すれば, 環境水温, 照度共に低かったことが, Hashimoto らの藻体で GTX3 の割合が顕著に高かった原因の 1 つと推察された. *A. tamiyavanichii* の毒組成は多様で, これまで採取地や培養条件の違いにより, PX1＋2 が 3 割程度と多いもの[7], GTX1＋4 が 6～9 割程度と非常に多いもの[9), 19), 22), 30), 31)], GTX2＋3 が 3～7 割程度と比較的多いもの[6), 9)]が報告されているが, いずれも GTX5 はおおむね 1 割以下であり, 本研究で用いた株のように, 4 割以上を占めた例は初めてである.

一方, 培養藻体の毒組成につき, Beppu ら[6]の培養藻体と比較すると, 副成分の組成には大きな差異があったが, GTX3 を主成分とする点では一致していた. 両者の培養条件は, 他の報告[7), 9), 19), 22), 30), 31)]に比べて低温度, 低照度でかつ明期時間が短いという特徴がある. 前述の Lim らの報告[30]に鑑みれば, このことも GTX3 の産生効率を高めた一因と推察された.

ムラサキイガイの毒成分組成は, おおむね *A. tamiyavanichii* 天然藻体のそれを反映したものであった. 1999 年の毒化事例[9]と比較しても, GTX4 の割合が少なく GTX5 の割合が高いという相違点が目立つ. このことに加え, 今回の調査で *A. tamiyavanichii* 以外の PSP 産生渦鞭毛藻が全く観察されなかったことから, 当該ムラサキイガイは *A. tamiyavanichii* により毒化したものと判断した.

HPLC 分析の結果から算出した毒力は, *A. tamiyavanichii* 培養藻体ではマウス毒性試験で測定した毒力の 1.07±0.21 (平均値±標準偏差) 倍となり, 両者はほぼ一致したが, *A. tamiyavanichii* 天然藻体では 1.39 および 1.40 倍, ムラサキイガイでは 1.80 倍と夾雑物の多い試料ほど大きなずれが見られた. PSP 同様ナトリウムチャンネルに作用するテトロドトキシン (TTX) では, マウス毒性試験において試料中に高濃度の塩化ナトリウムが存在するとマウスの致死時間が延び, 毒量が実際の値よりも低く見積もられることがある[32), 33)]. 毒力のずれの原因として, このような夾雑物の影響や HPLC 分析前処理中の低毒性成分から高毒性成分への変換 (特に GTX5 から STX への変換)[34)] などが考えられる.

今回, ムラサキイガイの毒化時に出現していた *A. tamiyavanichii* の細胞密度は, 最高でも 4,960 cell/L と別段高い水準ではなく, 同海域における過去の出現細胞密度[10)～15)]と同程度であった. したがって, *A. tamiyavanichii* が高い毒産生能を示す場合, その出現細胞密度が 5,000 cells/L 未満であっても, 二枚貝の毒化を引き起こす可能性が示唆される. また, 同じ海域であるにもかかわらず, 1999 年[9]と 2004 年 (本研究) に発生した *A. tamiyavanichii* では, 産生毒量や毒組成が大きく異なっていた. 今後, 遺伝的な変異や海洋環境の変化により, さらなる高毒量産生株の出現が懸念される. 以上のことより, これまで問題となってきた *A. tamarense* や *A. catenella* のみならず, 播磨灘に分布する *A. tamiyavanichii* も食品衛生上, 極めて危険な種であると結論した.

謝　辞

本研究は厚生労働科学研究費補助金に基づく研究成果の一部であり, 関係各位に深謝する.

文　献

1) Hashimoto, K., Noguchi, T. Recent studies on paralytic shellfish poison in Japan. Pure & Appl. Chem., **61**, 7-18 (1989).
2) Murakami, R., Noguchi, T. Paralytic shellfish poison. Shokuhin Eiseigaku Zasshi (J. Food. Hyg. Soc. Japan), **41**, 1-10 (2000).
3) Asakawa, M., Miyazawa, K., Noguchi, T. Studies on paralytic shellfish poison (PSP) toxification of bivalves in association with appearance of *Alexandrium tamarense*, in Hiroshima Bay, Hiroshima Prefecture. Shokuhin Eiseigaku Zasshi (J. Food. Hyg. Soc. Japan), **34**, 50-54 (1993).
4) Asakawa, M., Miyazawa, K., Takayama, H., Noguchi, T. Dinoflagellate *Alexandrium tamarense* as the source of paralytic shellfish poison (PSP) contained in bivalves from Hiroshima Bay, Hiroshima Prefecture, Japan. Toxicon, **33**, 691-697 (1995).
5) Asakawa, M., Takayama, H., Beppu, R., Miyazawa, K. Occurrence of paralytic shellfish poison (PSP)-producing dinoflagellate *Alexandrium tamarense* in Hiroshima Bay, Hiroshima Prefecture, Japan, during 1993-2004 and its PSP profiles. Shokuhin Eiseigaku Zasshi (J. Food. Hyg. Soc. Japan), **46**, 247-251 (2005).
6) Beppu, R., Nojima, K., Tsuruda, S., Gomez-Delan, G., Barte-Quilantang, M., Taniyama, S., Sagara, T., Nishio, S., Takayama, H., Miyazawa, K., Asakawa, M. Occur-

rence of PSP-producing dinoflagellate *Alexandrium tamiyavanichii* in Bingo-Nada, the central coastal water of the Seto Inland Sea, Hiroshima Prefecture, Japan. Mar. Pollut. Bull., **56**, 758–763 (2008).

7) Oh, S. J., Matsuyama, Y., Nagai, S., Itakura, S., Yoon, Y. H., Yang, H. S. Comparative study on the PSP component and toxicity produced by *Alexandrium tamiyavanichii* (Dynophyceae) strains occurring in Japanese costal water. Harmful Algae, **8**, 362–368 (2009).

8) Sakamoto, S., Kotani, Y. Variation of paralytic shellfish contents and composition in *Alexandrium tamarense* collected at Kure Bay, Hiroshima Prefecture. Bull. Nansei Natl. Fish. Res. Inst., **31**, 45–52 (1998).

9) Hashimoto, T., Matsuoka, S., Yoshimatsu, S., Miki, K., Nishibori, N., Nishio, S., Noguchi, T. First paralytic shellfish poison (PSP) infestation of bivalves due to toxic dinoflagellate *Alexandrium tamiyavanichii*, in the southeast coasts of the Seto Inland Sea, Japan. Shokuhin Eiseigaku Zasshi (J. Food. Hyg. Soc. Japan), **43**, 1–5 (2002).

10) Yoshimatsu, S., Ochi, Y., Ueda, T., Matsumoto, S., Yamanishi, S., Miki, K. "An annual report at 1999", ed. by Kagawa Akashiwo Research Institute, Kagawa Prefecture, 2001, p. 13–15.

11) Ochi, Y., Matsuoka, S., Yoshimatsu, S., Yamanishi, S., Miki, K. "An annual report at 2000", ed. by Kagawa Akashiwo Research Institute, Kagawa Prefecture, 2002, p. 13–15.

12) Ochi, Y., Matsuoka, S., Yoshimatsu, S., Yamanishi, S., Miki, K. "An annual report at 2001", ed. by Kagawa Akashiwo Research Institute, Kagawa Prefecture, 2003, p. 13–15.

13) Ochi, Y., Matsuoka, S., Yoshimatsu, S., Yamanishi, S., Miki, K. "An annual report at 2002", ed. by Kagawa Akashiwo Research Institute, Kagawa Prefecture, 2004, p. 14–16.

14) Honda, K., Matsuoka, S., Yoshimatsu, S., Miki, K. "An annual report at 2003", ed. by Kagawa Akashiwo Research Institute, Kagawa Prefecture, 2005, p. 14–16.

15) Honda, K., Ohyama, K., Yoshimatsu, S., Miki, K. "An annual report at 2004", ed. by Kagawa Akashiwo Research Institute, Kagawa Prefecture, 2006, p. 14–16.

16) Balech, E. Dinoflagelados nuevos o interesantes del Golfo de Mexico y Caribe. Rev. Mus. Argent. Cienc. Nat. "Ber. Rev.", **2**, 77–129 (1967).

17) Taylor, F., J., R., Fukuyo, Y., Larsen, J. "Manual on harmful marine microalgae", Hallegraeff, G. M., Anderson, D. M., Cembella, A. D. eds., France, UNESCO, 1995, p. 296–299.

18) Fukuyo, Y., Phoipunthin, P., Yoshida, K. *Protogonyaulax* (Dinophyceae) in the Gulf of Thailand. Bull. Plankton Soc. Jpn., **35**, 9–20 (1988).

19) Kodama, M., Ogata, T., Fukuyo, Y., Ishimaru, T., Wissessang, S., Saitanu, K., Panichyakarn, V., Piyakarnchana, T. *Protogonyaulax cohorticula*, a toxic dinoflagellate found in the Gulf of Thailand. Toxicon, **26**, 707–712 (1988).

20) Phanichyakarn, V., Wisessang, S., Piyakarnchana, T., Fukuyo, Y., Ishimaru, T., Kodama, M., Ogata, T. Ultrastructure of *Alexandrium cohorticula* found in the Gulf of Thailand. Toxic Phytoplankton Blooms in the Sea. Smayda, T. J., Shimizu, Y. eds., Elsevier, Amsterdam, 1993, p. 165–168.

21) Usup, G., Pin, L. C., Ahmad, A., Teen, L. P. Phylogenetic relationship of *Alexandrium tamiyavanichii* (Dinophyceae) to other *Alexandrium* species based on ribosomal RNA gene sequences. Harmful Algae, **1**, 59–68 (2002).

22) Ogata, T., Pholpunthin, P., Fukuyo, Y., Kodama, M. Occurrence of *Alexandrium cohorticula* in Japanese coastal water. J. Appl. Phycol., **2**, 351–356 (1990).

23) 岡市友利, 西尾幸郎, 今富幸也. 2. 有毒プランクトン研究法—試料の採集と培養. 有毒プランクトン—発生・作用機構・毒成分. 恒星社厚生閣, 東京, 1982, p. 22–34.

24) Watanabe, M. M., Miroki, M., Simizu, A., Erata, M., Mori, F., Sakurai, Y. NIES-collection, List of strains, Fifth edition, Microalgae and Protozoa. National Institute for Environmental Studies, Tsukuba, 1997, p. 140.

25) 大島泰克. 第7章自然毒・A動物毒・3. 麻痺性貝毒. 食品衛生検査指針理化学編 (厚生労働省監修), 日本食品衛生協会, 東京 (2005), p. 673–680.

26) Oshima, Y. Manual on Harmful Marine Microalgae. Hallegraeff, G. M., Anderson, D. M., Cembella, A. D. eds., Paris, France, UNESCO, 1995, p. 81–94.

27) Arakawa, O., Noguchi, T., Onoue, Y. Paralytic shellfish toxin profiles of xanthid crabs *Zosimus aeneus* and *Atergatis floridus* collected on reefs of Ishigaki Island. Fish. Sci., **61**, 659–662 (1995).

28) Hashimoto, T., Nishio, S., Nishibori, N., Yoshioka, S., Noguchi, T. A new analytical method for gonyautoxins based on postculmn HPLC. Shokuhin Eiseigaku Zasshi (J. Food. Hyg. Soc. Japan), **43**, 144–147 (2002).

29) Sekiguchi, K., Ogata, T., Kaga, S., Yoshida, M., Fukuyo Y., Kodama, M. Accumulation of paralytic shellfish toxins in the scallop *Patinopecten yessoensis* caused by the dinoflagellate *Alexandrium catenella* in Otsuchi Bay, Iwate Prefecture, northern Pacific coast of Japan. Fish. Sci., **67**, 1157–1162 (2001).

30) Lim, P.-T., Leaw, C.-P., Usup, G., Kobiyama, A., Koike, K., Ogata, T. Effects of light and temperature on growth, nitrate uptake, and toxin production of two dinoflagellates: *Alexandrium tamiyavanichii* and *Alexandrium minutum* (Dinophyceae). J. Phycol., **42**, 786–799 (2006).

31) Wissessang, S., Ogata, T., Kodama, M., Fukuyo, Y., Ishimaru, T., Saitanu, K., Yongvanich, T., Piyakarnchana, T. Accumulation of paralytic shellfish toxins by green mussel *Perna viridis* by feeding on cultured cells of *Alexandrium cohorticula* isolated from the Gulf of Thailand. Nippon Suisan Gakkaishi, **57**, 127–131 (1991).

32) Ozawa, C. Detoxication of poisonous puffer roe pickled in rice bran. I. Toxicity of puffer roe pickled in rice bran. Shokuhin Eiseigaku Zasshi (J. Food. Hyg. Soc. Japan), **24**, 258–262 (1983).

33) Shimada, K., Ohtsuru, M., Nigota, K. Effects of coexisting materials on the mouse bioassay method for the determination of tetrodotoxin. Shokuhin Eiseigaku Zasshi (J. Food. Hyg. Soc. Japan), **26**, 507–510 (1985).

34) Nagashima, Y., Sato, Y., Noguchi, T., Fuchi, Y., Hayashi, K., Hashimoto, K. Paralytic shellfish poison in the "hiogi" scallop *Chlamys nobilis*. Mar. Biol., **98**, 243–246 (1988).

Special Topic 5

無毒フグの養殖

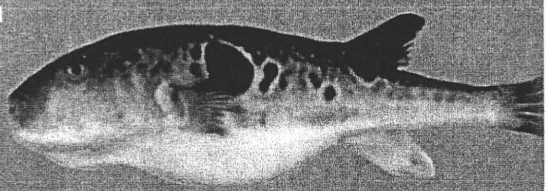

長崎大学水産学部
荒川 修

Key words　テトロドトキシン／フグ中毒／トラフグ／網生け簀養殖／構造改革特区

はじめに

フグの肝(きも)は致死的な毒を持つにもかかわらず、かつては「秘伝の毒抜き」を施したうえ、多くの食通が好んで食していた。しかし食中毒も後を絶たず、近年に至るまで多数の人命が奪われてきた。なかでも1975年に8代目坂東三津五郎が好物のトラフグの肝を食べて急死した事件はあまりにも有名だ。この事件では、調理師が逮捕され有罪となったが、1983年12月に厚生省(現厚生労働省)は「フグの衛生確保について」の通知を出し、すべてのフグの肝を食用に供することを禁止した。

一方、フグ毒は有毒餌生物由来であり、これを遮断して無毒の餌で養殖すれば、肝も無毒になることがわかってきた。

本稿では、フグ毒やフグの毒化機構にかかわる科学的知見について解説するとともに、無毒トラフグの養殖とフグ肝食用解禁への取り組みについて紹介する。

フグ毒テトロドトキシン(TTX)の正体[1)]

フグ毒は、正式にはテトロドトキシン(TTX)という(図1)。TTXは分子量319の神経毒で、毒力は青酸ソーダの約1000倍もある。高純度のTTXは各種の有機溶媒と水に不溶性を示すが、酸を加えると水には溶ける。しかし、中性と弱酸性溶液中では安定で、熱にも強く、煮たり、焼いたりといった通常の加熱調理では分解しない。

毒力は5,000～6,000 MU/mg(MU＝マウスユニット)。TTXの場合、1 MUは腹腔内投与により体重20 gのマウスを30分で死亡させる毒量で、ヒト(体重50 kg)に対する最小致死量は10,000 MU(約2 mg)程度と推定されている。

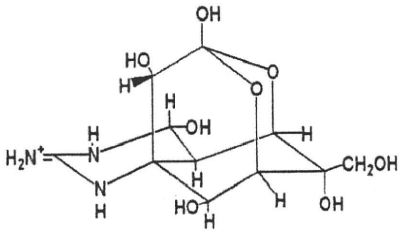

図1　TTXの化学構造
TTXは低分子(分子量319)の神経毒で、化学構造は1964年に日米の3つの研究グループによりほぼ同時に決定された。

天然フグの肝で食中毒におちいると、食後20分～3時間で舌の先や四肢に痺れや頭痛・腹痛、歩行困難などの症状が現れ、重篤な場合は呼吸麻痺で死亡する。TTXに対する解毒剤や特効薬はなく、食べた物を吐き出させ、人工呼吸器の使用により呼吸循環系を適切に管理する以外、これといった治療法はない。

TTXはごく低濃度で神経や筋細胞の膜表面にあるナトリウムチャネル(ナトリウムが透過する通路)を選択的に塞ぎ、活動電位の伝導を阻害する。ナトリウムチャネルを特異的にブロックするTTXの特徴は、主

Author 著者

荒川 修(あらかわ おさむ)
長崎大学水産学部 教授

1989年3月、東京大学大学院農学系研究科博士課程修了。農学博士。米国ノースウエスタン大学医学部研究助手、鹿児島大学水産学部助手、長崎大学水産学部助教授を経て、2002年4月より現職に。専門は食品衛生学、水産化学。無毒フグの生産と肝の食用化、フグ毒保有生物の毒化機構などを研究中。内閣府食品安全委員会専門委員、日本水産学会九州支部評議員。

に神経生理学分野の研究で重要な役割を担い、中国では臨床用医薬(末期がん患者の鎮痛薬)としても用いられているという。日本でも以前は神経痛とリウマチの止痛薬として臨床応用されていた。

TTXを持つ魚介類

日本近海に生息する海産フグのなかでは、フグ科に属するクサフグ、コモンフグ、ショウサイフグ、マフグ、トラフグなど少なくとも22種がTTXを持つ有毒種とされている[1,2]。ハリセンボン科やハコフグ科のフグはまったくTTXを持たない。

有毒部位は種によって異なるが、一般に内臓、とくに肝臓と卵巣は強毒(100～999 MU/g)ないし猛毒(1000 MU/g以上)の場合が多く、これらの部位の食用はすべてのフグ類で禁じられている。なお、食用可能な部分も次に示しておく。

①トラフグ、サバフグなどは筋肉、精巣、皮は無毒(10 MU/g未満)で食用可能。
②ショウサイフグ、マフグなどは皮にも毒があり、筋肉と精巣のみ食用可能。
③クサフグ、コモンフグなどは精巣も有毒で、筋肉のみ食用可能。
④ドクサバフグ、オキナワフグなどは筋肉にも毒があり、食用にならない。

TTXはフグに特有の毒と思われていたが、1964年にカリフォルニアイモリの毒がTTXと同定されて以来、ツムギハゼ、アテロパス属のカエル、ヒョウモンダコ、肉食性巻貝ボウシュウボラ、腐肉食性の小型巻貝類、モミジガイ属のヒトデ、オウギガニ科の有毒ガニ、マルオカブトガニ、ヒラムシ類、ヒモムシ類など、多様な生物にTTXが見出されてきた。さらに1980年代後半には、TTXがある種の海洋細菌によってつくられることが示された。

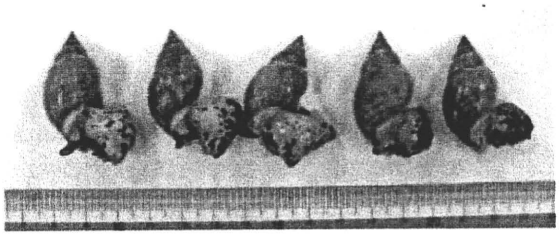

図2 腐肉食性巻貝キンシバイ
2007年7月に長崎市、2008年7月には熊本県天草市で重篤な食中毒を引き起こした。内臓だけでなく筋肉にも多量のTTXを保有する。

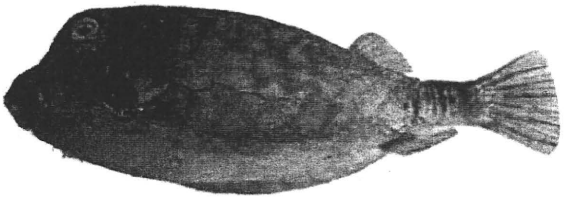

図3 ハコフグ
長崎県五島列島では、郷土料理として長年ハコフグの味噌焼きが食されてきたが、2001年から2008年にかけ、同列島を含む西日本でこれによる中毒が立て続けに6件発生した。

フグ毒による食中毒[1)]

厚生労働省の統計によれば、2001年から2009年までの9年間で309件のフグ中毒が発生し、23名が命を落としている。これらの食中毒事件は、素人が自分で釣ったフグや譲り受けたフグを家庭で調理し、肝臓や卵巣などの猛毒部位を食べたケースがほとんどで、専門店での事故は少ない。また、養殖トラフグによる中毒事例もない。

では、海外ではどうだろう？ 中国や台湾では日本ほど頻繁にはフグを食べないが、それでも天然フグによる中毒事例が発生している。なかには、からすみ(ボラ卵巣の塩蔵品)の模造品として売られていたフグの卵巣や、カワハギの肉として販売されていた有毒フグの乾燥魚肉を食べて中毒したケースもある。

また、フグ以外の魚介類によるTTX中毒の例もある。中国や台湾では昔からアラレガイ、ハナムシロガイ類縁種などの小型巻貝類を食べる習慣があり、食中毒が頻発している。

日本でも2007年7月に長崎市で、2008年には熊本県天草市でキンシバイという小型巻貝(図2)による食中毒事件が発生した。

一方、タイやカンボジアなど東南アジアの一部の国ではカブトガニの卵を食材として利用しており、TTXによる食中毒が希に発生している。

その他、日本では前出の肉食性大型巻貝ボウシュウボラ、台湾ではツムギハゼによるTTX中毒の事例がある。

他方、TTXとは異なる毒を持つフグによる中毒例もある。2001年11月から2008年10月にかけ、三重、宮崎、長崎の各県で、ハコフグ(図3)の味噌焼きによる中毒が立て続けに6件発生し、計10名が中毒、うち1

名が死亡した。

ハコフグ中毒はミオグロビン尿症や血清クレアチンホスホキナーゼ(CPK)値の異常な上昇を伴う激しい筋肉痛がみられる点、ならびに発症から死亡もしくは回復に至るまでの時間経過が比較的長いという点で、日本で希に起こるアオブダイ中毒に酷似しており、パリトキシン(PTX)様毒が原因物質と考えられる。

バングラデシュ産淡水フグもPTX様毒を保有し、同国で頻繁に食中毒を起こしている。

一方、東南アジアの河川や湖沼に生息する淡水産の小型のフグは、主に皮に麻痺性貝毒(PSP)を保有しており、タイやカンボジアでは時にこれによる食中毒が発生して死者も出ている。PSPはある種の植物プランクトンが産生する一群の神経毒で、主要成分のサキシトキシン(STX)は分子の大きさや毒力、作用機序がTTXとほぼ等しい。米国フロリダ産のヨリトフグ属のフグも筋肉に多量のPSPを保有しており、米国では2002年から2004年にかけて28例の食中毒を起こしている。

フグの毒化機構[2,3]

本題に入る前に、TTXの検出・定量法について簡単にふれておく。厚生労働省編集の「食品衛生検査指針」には、参考法としてマウス毒性検査法が記載されている。本法では、試料(フグ組織など)を0.1%酢酸水溶液で加熱抽出し、得られた抽出液をマウス(ddY系、雄、体重20 g)の腹腔内に投与して、その致死時間から毒力を算出する。毒力を表す単位として、前出のMUが用いられる。本法の検出限界は、特別に濃縮操作を行わない限り2～10 MU/gである。一方、機器を用いる分析法としては、以前は主に高速液体クロマトグラフィー(HPLC)蛍光分析が行われていたが、近年ではさらに簡便で特異性の高い液体クロマトグラフィー質量分析法(LC/MS法)が普及してきた。この方法では、マウス毒性検査法と同様の抽出液について、限外ろ過などの前処理を施したうえ分析装置に導入する。検出限界は0.1 MU/g程度で、より高感度の分析が可能である。

以上のような手法の確立や応用を含め、多くの研究者が長年にわたってフグ毒研究を行ってきた。その過程で、明らかになっていることを以下にまとめる。

①フグの毒性には著しい個体差や地域差がみられる。

②TTXは小型巻貝、ヒトデ、ヒラムシ、ヒモムシなどフグ以外の生物(フグの餌生物)にも広く分布する。

③大型巻貝ボウシュウボラは有毒ヒトデを食べることでTTXを蓄積する。

④孵化稚魚のときから無毒の餌を与えて人工的に飼育したトラフグやクサフグは毒を持たないが、これらのフグにTTXを経口投与すると効率よくこれを蓄積する。

⑤TTXは海洋細菌が産生している。

以上が順次明らかとなり、「フグは自分自身で毒をつくるのではなく、細菌を起源とし、食物連鎖を介して生物濃縮された毒を有毒餌生物から得ている」というフグの毒化外因説が有力視されるようになった。

この説にもとづけば、有毒餌生物を完全に遮断した状態で、無毒の餌を与えて飼育する「囲い養殖法」で養殖すれば無毒のフグができると考えられる。

2000年以降、筆者らはフグの養殖や流通、販売などにかかわる複数の業者から相次いで「自分たちが扱っている養殖フグの毒性を調べて欲しい」との要請を受けた。彼らは経験的に自分たちのフグが肝も無毒であることを知っており、科学的な裏付けを得ることで、それらの販売を可能にしたいと考えていた。

養殖トラフグの肝は大きく、体重の2～3割を占める。費用をかけて焼却処分しなければならないこの部位を有効利用することができれば、低迷が続く関連業者の経営が大きく改善される。また同時に「フグ肝食」という1983年の規制以降姿を消すこととなった日本独自の食文化を復活させることもできる。

筆者らは、前述の業者らと共同で日本の主要なフグ養殖地(長崎、佐賀、熊本、鹿児島、愛媛、和歌山、静岡の7県)から囲い養殖されたトラフグ当歳(0歳)～3年魚(2歳)計約5,000個体を集め、マウス毒性検査法により主に肝臓の毒性を調査した。さらに、一部の個体についてはLC/MS分析により微量なTTXの有無についても検討した。その結果、いずれの個体からも毒性あるいはTTXは検出されず、「フグの毒化は餌生物由来であること」、ならびに「囲い養殖により肝も無毒のフグが生産可能であること」が実証された。

一方、有毒餌生物を介してフグ体内に取り込まれた後のTTXの存在形態や動態に関しては、いまだに不明な部分が少なくない。

最近、筆者らは、トラフグの無毒養殖個体の筋肉にTTXを注射投

与すると、血液を介して速やかにTTXが肝臓に移行することを見出した。また、海産フグ肝臓の培養組織が*in vitro*で顕著にTTXを取り込むとの報告もある。無毒の一般魚ではこのような現象はみられず、明らかにフグの肝臓には特異なTTX蓄積機構が存在する。関連して、海産フグの血漿中にはTTX結合性タンパク質の存在が見出されており、このような高分子物質がTTXの輸送や蓄積に深くかかわっているものと推察される。

他方、TTXを保有する有毒海産フグやツムギハゼ、スベスベマンジュウガニ、ニホンイモリはTTXに対して極めて高い抵抗性を示す。すなわち、これらの生物に腹腔内投与した場合のTTXの最小致死量は、マウスの300～1000倍（イモリでは1万倍以上）に達する。これに対し、無毒の海産フグは中程度、一般魚はマウスと同程度の低い抵抗性を示す。有毒フグやイモリのTTX抵抗性発現メカニズムの1つとして、彼らがTTX耐性型のナトリウムチャネルを保有していることがあげられる。

「囲い養殖法」で無毒フグを生産[3)]

トラフグ養殖は、まず種苗生産からはじまる。一般に、天然の雌から得た卵に、雄の養殖魚の精子をかけて人工授精させ、孵化した仔魚は、体長が20 mm程度を超えるまで1～2か月間、屋内水槽中でアルテミアやワムシ、人工飼料などを与えて飼育する。この間、天然魚由来の受精卵に含まれるTTXは、ほぼそのまま孵化仔魚に受け継がれるが、仔魚の生長とともに相対的な含量が下がり、1週間程度でマウス毒性検査法では検出できなくなる。その後は、沖出しして海面の網生け簀に移し、市販の魚粉やアジ、サバ、アミなどの生餌を与えて出荷サイズ〔通常1 kg（2年魚）〕になるまで飼育を続ける。

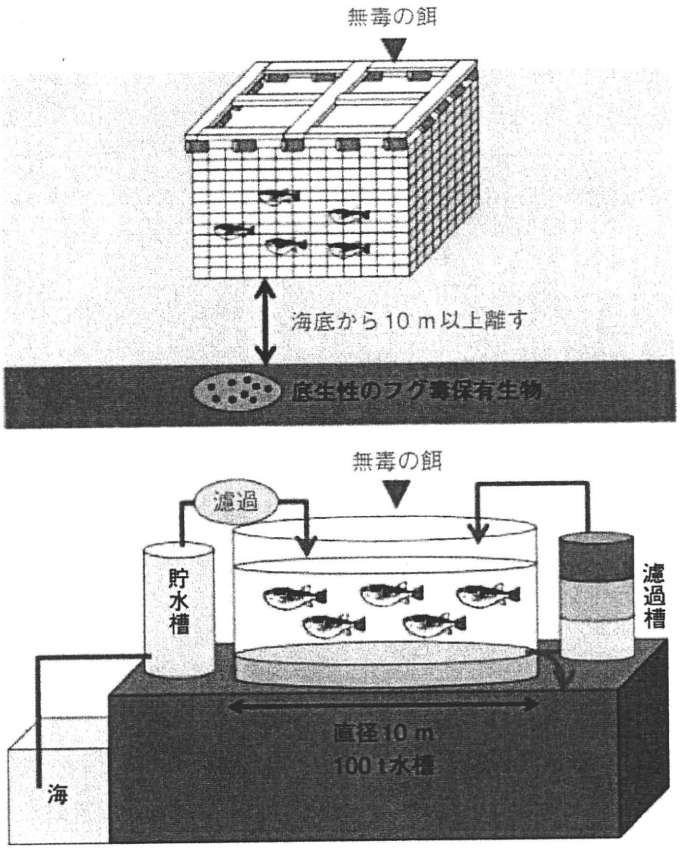

図4 「囲い養殖法」による無毒フグの生産

底生性の有毒餌生物を遮断し、無毒の餌を与えて飼育する「囲い養殖法」により無毒のフグを生産することができる。網生け簀養殖（上）と陸上養殖（下）の2つの形態がある。

最近では、沖出しせず、屋内の大型水槽で飼育する陸上養殖も盛んになってきた。この方法には、極めて高コストという難点もあるが、水質や水温などの管理が容易で、寄生虫も排除できるという大きなメリットがある。

「囲い養殖法」は、前述のとおり、フグを網生け簀で飼育し、有毒餌生物を遮断した状態で、無毒の餌を与えて飼育する養殖方法である（図4上）。

網目のサイズに規定は設けられていないが、網の底を海底から10 m以上離すこと、陸上養殖（図4下）では、ろ過海水もしくは人工海水を使用することを必要条件としている。

しかし、こうした方法は必ずしも特殊というわけではなく、日本で行われているトラフグ養殖は、ほとんどがこの形態に当てはまる。

現在、トラフグ市場では養殖ものが8～9割を占めるといわれている。したがって日本で流通している国産のトラフグは、ほとんどが肝も無毒ということになる。

とはいえ、網で仕切った湾（かつて日本で行われていた）や海水をろ過せずに汲み入れた陸上の養殖池で行う（現在、中国で行われている）粗放的な養殖では、養殖フグであっても毒を持つ可能性があり、素人判断で安易に肝を食するのはきわめて危険である。

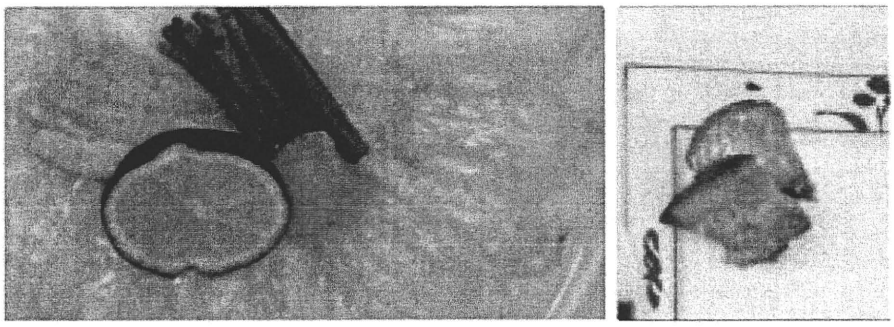

図5　フグ肝料理
毒性検査で無毒を確認したフグ肝を調理し、試食会を行った。左はフグ刺しと肝刺し、右は肝の西京焼き。いずれも好評で、肝の食用解禁を期待する多くの声をいただいた。

フグ肝食用解禁への取り組み[3)]

筆者らが業者と行った共同研究の成果にもとづき、2004年6月、佐賀県と嬉野町(現・嬉野市)は内閣官房構造改革特区推進室に「佐賀・嬉野温泉ふぐ肝特区」構想を提案した。この構想では、マイクロタグによる生産管理システムを導入。さらに、中間の流通を排除し、特定の業者が囲い養殖したトラフグの肝を嬉野町内の特定の飲食店に直接出荷し、そこでのみ消費するという形態をとることで、有毒フグ肝の混入を防ぎ、安全・安心なフグ肝食の確立を図ろうとした。

しかし、内閣府食品安全委員会の審議では、「餌生物以外の要因(とくにフグ毒産生細菌)による毒化の可能性を否定できない」、「安全性を判断するには科学的データが不十分」などの意見が出され、最終的に厚生労働省は、規制解除を認めなかった。

その後、2005年から2009年にかけ、東京の服部栄養専門学校と長崎の川島学園九州調理師専門学校において、それぞれ数回「フグ料理を楽しむ会」を実施した。そこでは、通常のフグ刺し、フグちりなどに加え、全個体の毒性検査(無毒の確認)を前提として肝刺し、肝の西京焼き、肝入り茶碗蒸しなどの肝料理(図5)を出し、参加者には「自己責任」においてそれらを味わっていただいた。

フグ肝はアンコウやカワハギの肝より濃厚で、そのまったりとした味と食感は、世界三大珍味のフォアグラに勝るとも劣らない。最初はこわごわであっても一度口にすれば恐怖感は消え、肝なしでは淡泊な一般のフグ料理が物足りなく思えてくる。参加者の方々からは「フォアグラのようだ！」「コクがあって美味い！」などと肝料理に対する高評価、肝の食用解禁を期待する多くの声をいただいた。

おわりに

2010年3月、佐賀県は、嬉野市から唐津市に対象を変え、陸上養殖された約4000個体のフグの肝がすべて無毒であったとのデータを添えて、再びフグ肝特区構想を提案した。今回の提案では、囲い養殖の方法を、より厳密に管理が可能な陸上養殖に限定し、さらに適切な毒性検査を実施したうえで無毒が確認できた肝を提供するとした。残念ながら今回の構想も認可を得るには至らなかったが、県の担当者の話では、前回とは異なり厚生労働省も一定の理解を示しており、現在、同省と相談しながら特区とは別の形でのフグ肝食用化の方策を模索中という。

日本人は、昔からフグを好み、命がけで独自のフグ食文化を築きあげてきた。無毒フグ肝の食用が可能となれば、未利用水産資源が有効利用され、地域振興や水産業の活性化に大きく貢献するばかりでなく、世界に誇れる食文化のひとつとなり得る。日本人が食へのこだわりと好奇心を失わない限り、いずれはこのような光景が現実のものとなるであろう。

[参考文献]

1) 荒川修ほか：公衆衛生，73：323-327，2009.
2) 荒川修，野口玉雄：化学療法の領域，24：92-101，2008.
3) 荒川修ほか：ジャパンフードサイエンス，44：42-47，2005.

THE JOURNAL OF BIOLOGICAL CHEMISTRY VOL. 285, NO. 17, pp. 13079–13091, April 23, 2010

Poly(ADP-ribose) Polymerase (PARP)-1-independent Apoptosis-inducing Factor (AIF) Release and Cell Death Are Induced by Eleostearic Acid and Blocked by α-Tocopherol and MEK Inhibition*[S]

Received for publication, July 14, 2009, and in revised form, February 2, 2010 Published, JBC Papers in Press, February 22, 2010, DOI 10.1074/jbc.M109.044206

Kazunari Kondo[‡1], Saemi Obitsu[‡], Sayaka Ohta[‡], Katsuyoshi Matsunami[§], Hideaki Otsuka[§], and Reiko Teshima[‡]

From the [‡]Division of Novel Food and Immunochemistry, National Institute of Health Sciences, 1-18-1 Kamiyoga, Setagaya, Tokyo 158-8501 and the [§]Department of Pharmacognosy, Graduate School of Biomedical Sciences, Hiroshima University, 1-2-3 Kasumi, Minami-ku, Hiroshima 734-8553, Japan

Poly(ADP-ribose)polymerase-1 (PARP-1) is thought to be required for apoptosis-inducing factor (AIF) release from mitochondria in caspase-independent apoptosis. The mechanism by which AIF is released through PARP-1 remains unclear. Here, we provide evidence that PARP-1-independent AIF release and cell death are induced by a trienoic fatty acid, α-eleostearic acid (α-ESA). α-ESA induced the caspase-independent and AIF-initiated apoptotic death of neuronal cell lines, independently of PARP-1 activation. The cell death was inhibited by the MEK inhibitor U0126 and by knockdown of MEK using small interfering RNA. However, inhibitors for JNK, p38 inhibitors, calpain, phospholipase A_2, and phosphatidylinositol 3-kinase, did not block cell death. AIF was translocated to the nucleus after the induction of apoptosis by α-ESA in differentiated PC12 cells without activating caspase-3 and PARP-1. The α-ESA-mediated cell death was not inhibited by PARP inhibitor 3,4-dihydro-5-[4-(1-piperidinyl)butoxyl]-1(2*H*)-isoquinoline and by knockdown of PARP-1 using small interfering RNA. Unlike *N*-methyl-*N*′-nitro-*N*-nitrosoguanidine treatment, histone-phosphorylated histone 2AX was not phosphorylated by α-ESA, which suggests no DNA damage. Overexpression of Bcl-2 did not inhibit the cell death. α-ESA caused a small quantity of superoxide production in the mitochondria, resulting in the reduction of mitochondrial membrane potential, both of which were blocked by a trace amount of α-tocopherol localized in the mitochondria. Our results demonstrate that α-ESA induces PARP-1-independent AIF release and cell death without activating Bax, cytochrome *c*, and caspase-3. MEK is also a key molecule, although the link between ERK, AIF release, and cell death remains unknown. Finding molecules that regulate AIF release may be an important therapeutic target for the treatment of neuronal injury.

Apoptosis is a mode of programmed cell death that is used by multicellular organisms to remove surplus and unwanted cells in the immune and nervous systems (1–5). Apoptosis is characterized by cell detachment, cell shrinkage, chromatin condensation, DNA degradation, and plasma membrane blebbing (5–7). The surplus cells are removed by caspases, which are key effector molecules of apoptotic cell death. Apoptosis is activated through two main pathways as follows: the extrinsic pathway, which originates from the activation of cell-surface death receptors, such as Fas and tumor necrosis factor-receptor 1, and results in the activation of caspase-8; and the intrinsic pathway, which originates from the mitochondrial release of cytochrome *c* and results in the activation of caspase-9 through the Cyt-c[2]/apoptotic protease-activating factor-1/procaspase-9 heptamer (5, 8, 9). Most apoptotic stimuli use a mitochondrion-dependent process such as membrane potential shutdown and outer membrane permeabilization controlled by Bax and Bak, which are pro-apoptotic members of the Bcl-2 family (6–9). This results in the release of the pro-apoptotic protein Cyt-c, which triggers caspase activation, or the apoptosis-inducing factor (AIF), which triggers caspase-independent pathways, from mitochondrial intermembrane space.

In the developing nervous system, apoptosis is necessary for the establishment of appropriate cell numbers and for the elimination of unwanted cells (10); however, in the adult nervous system, the inappropriate induction of apoptotic cell death contributes to neurodegenerative diseases (15, 16). Activation of the mitochondrial signaling cascade can activate both caspase-dependent and caspase-independent apoptosis (11, 12). AIF is a key molecule in caspase-independent neuronal cell death (13–16). AIF is released from the mitochondria into the cytosol and then translocated to the nucleus in response to neuronal

* This work was supported by grants from the Ministry of Health, Labor, and Welfare of Japan, the Japan Health Sciences Foundation, and Grant-in-aid for Scientific Research 20590132 (to K. K.).

[S] The on-line version of this article (available at http://www.jbc.org) contains supplemental Figs. S1 and S2 and Movie S1.

[1] To whom correspondence should be addressed. Tel.: 81-3-3700-1141; E-mail: kondo@nihs.go.jp.

[2] The abbreviations used are: Cyt-c, cytochrome *c*; α-ESA, α-eleostearic acid; MEK, mitogen-activated protein kinase kinase; JNK, c-Jun N-terminal kinase; ERK, extracellular signal-regulated kinase; γ-H2AX, phosphorylated histone 2AX; AIF, apoptosis-inducing factor; Bak, Bcl-2-antagonist/killer; Bax, Bcl-2-associated X protein; CPT, camptothecin; DPQ, 3,4-dihydro-5-[4-(1-piperidinyl)butoxyl]-1(2*H*)-isoquinoline; ERK, extracellular signal-regulated kinase; MEK, mitogen-activated protein kinase kinase; MNNG, *N*-methyl-*N*′-nitro-*N*-nitrosoguanidine; NGF, nerve growth factor; PARP-1, poly(ADP-ribose) polymerase-1; Z-, *N*-benzyloxycarbonyl; fmk, fluoromethyl ketone; ROS, reactive oxygen species; α-ESA, α-eleostearic acid; Ab, antibody; siRNA, small interfering RNA; TUNEL, terminal dUTP nick end-labeling; α-Toc, α-tocopherol; NMDA, *N*-methyl-D-aspartic acid; STS, staurosporine; JNK, c-Jun N-terminal kinase; PAR, polymer of ADP-ribose; CM-H2DCF-DA, 5(and 6)-chloromethyl-2′,7′-dichlorodihydrofluorescein diacetate; NBD, 7-nitro-2,1,3-benzoxadiazol-4-yl.

stimuli, including hypoxia, cerebral ischemia, and *N*-methyl-*N*′-nitrosoguanidine (MNNG) or *N*-methyl-D-aspartic acid (NMDA) insult (15, 17–20). Poly(ADP-ribose) polymerase-1 (PARP-1) activation is required for the translocation of AIF in fibroblasts (20). Moubarak *et al.* (21) has reported that the sequential activation of PARP-1, calpain, and Bax is essential in AIF-mediated programmed necrosis.

α-Eleostearic acid (α-ESA) is a conjugated trienoic fatty acid that occurs in the seeds of plants such as *Vernicia* spp. α-ESA has been reported to suppress tumor growth through caspase-3 and peroxisome proliferator-activated receptor-γ activation accompanied by DNA fragmentation (22–24). Recently, we have found that α-ESA induces caspase-independent apoptosis that is not associated with nucleosomal DNA fragmentation in neuronal cells. Notably, α-ESA-mediated apoptotic cell death is accompanied by AIF translocation to the nucleus and prolonged ERK phosphorylation that lasts for more than 16 h, but not by PARP-1 activation, in rat adrenal pheochromocytoma PC12 cells. The MEK inhibitor U0126 and a trace amount of α-tocopherol (α-Toc) completely inhibited the apoptotic cell death. The methyl ester of α-ESA (α-ESA-Me) did not induce apoptotic cell death, even though it has the same conjugated triene group as α-ESA. Here, we show that α-ESA causes PARP-1-independent AIF release and the cell death through the superoxide production in a small quantity in the mitochondria and the prolonged ERK1/2 phosphorylation without inducing other apoptotic molecules such as Bax, Bcl-2, Cyt-c, caspase-3, and PARP-1.

EXPERIMENTAL PROCEDURES

Cell Culture—PC12 (JCRB0266) cells were grown in Dulbecco's modified Eagle's medium supplemented with 10% horse serum and 5% fetal calf serum, penicillin, and streptomycin (Invitrogen). Human neuroblastoma (SH-SY5Y) cells (American Type Culture Collection (ATCC), CRL-2266) were grown in Dulbecco's modified Eagle's medium/F-12 supplemented with 10% fetal calf serum. Mouse neuroblastoma × rat glioma hybrid (NG108-15) cells (ATCC, HB-12317) were grown in Dulbecco's modified Eagle's medium supplemented with 10% fetal calf serum. The PC12 cells were induced to differentiate by treatment with 50 ng/ml NGF 7 S (Sigma) and were maintained at 37 °C and 5% CO_2. The SH-SY5Y and NG108-15 cells were induced to differentiate by treatment with 10 μM all-*trans*-retinoic acid (Sigma) and 250 μM dibutyryl cyclic AMP (Tocris), respectively. The PC12 and NG108-15 cells were allowed to differentiate on polylysine-coated plates or glass chambers. The cell viability was measured by a WST-8 assay (Nacalai Tesque, Japan). Briefly, PC12 cells were differentiated by NGF for 48 h, and then α-ESA was added to the cells. Sixteen hours later, the cell count reagent (2-(2-methoxy-4-nitrophenyl)-3-(4-nitrophenyl)-5-(2,4-disulfophenyl)-2*H* tetrazolium) for the WST-8 assay was added to the cells, and the cells were incubated for 1–2 h. For proliferating cells, α-ESA was added 16–18 h after seeding the cells. Cell viability was measured by 450 and 650 nm (as a reference) absorbance. When pretreatment with a specific inhibitor is needed, an inhibitor was added to the cells 30 min before α-ESA. Cell viability data were obtained between two and four independent experiments performed in triplicate.

Antibodies and Chemicals—The Abs for ERK, phospho-ERK, JNK/stress-activated protein kinase, phospho-JNK/stress-activated protein kinase, p38, phospho-p38, Akt, phospho-Akt, caspase-3, MEK1 (61B12), Bcl-2, and glyceraldehyde-3-phosphate dehydrogenase (14C10) were purchased from Cell Signaling. The Abs for AIF (E-1), Cyt-c (7H8), Bax (N-20), Bcl-2 (C-2), and PARP-1 (H-250) were purchased from Santa Cruz Biotechnology. Anti-PAR (10H) was obtained from Alexis Biochemicals. Anti-H2A was obtained from Millipore. Anti-γ-H2AX was obtained from Active Motif. Anti-manganese superoxide dismutase was obtained from Assay Designs. Anti-MEK2 was purchased from BD Biosciences. The pan-caspase inhibitor Z-VAD-fmk, PD98059, SB203580, U0126, palmitoyl trifluoromethyl ketone, and DPQ were obtained from Calbiochem. SP600125 was obtained from Assay Designs. 7-Nitro-2,1,3-benzoxadiazol-4-yl (NBD)-labeled α-Toc was kindly provided by J. Atkinson (Brock University, Canada). Bromoenol lactone and methylarachidonyl fluorophosphates were purchased from Cayman Chemicals. The orange fluorescent protein-tagged leader sequence of E1α pyruvate dehydrogenase (Organelle Light), MitoTracker Red CM-H2Ros, and MitoSOX Red were purchased from Invitrogen and used to stain with the mitochondria. The high purity of α-ESA was purchased from Larodan Fine Chemicals (Sweden). Staurosporine was obtained from Tocris Bioscience. 5(and 6)-Chloromethyl-2′,7′-dichlorodihydrofluorescein diacetate (CM-H2DCF-DA) was purchased from Invitrogen. BESSo-AM was purchased from Wako Pure Chemicals (Japan). α-ESA-Me was prepared by reacting α-ESA with trimethylsilyl-diazomethane in 10% hexane solution (TCI, Japan). Trimethylsilyl-diazomethane was added to the reaction mixture (α-ESA, 20.0 mg in 18 ml methanol) drop-by-drop over 1 h at room temperature to avoid by-products. The reaction mixtures were purified with a C_{18} column. The resulting material was stored in a vial under a nitrogen gas atmosphere at −80 °C or below.

Western Blot Analysis—PC12 cells were cultured at 6×10^5 cells/dish in 10-cm poly-L-lysine-coated dishes in a differentiation condition. After 24 h, the cells were cultured with NGF for another 48 h. α-ESA was then added to the cells to induce apoptosis after inhibitors, U0126 or α-Toc, if needed. The cells were collected after 16 h of α-ESA treatment. Briefly, after the cells were washed with Tris-buffered saline, lysates were prepared using Triton-based lysis buffer containing protease inhibitors and phosphatase inhibitors. Neurotropic factor (NGF) was included in the washing buffer to avoid other types of apoptosis caused by neurotropic factor withdrawal from differentiating cells. A ProteoExtract subcellular proteome extraction kit (Calbiochem) was used for the preparation of the nuclear and cytosolic fractions. The cell lysates and subcellular fraction samples were resolved by SDS-PAGE on 5–20% gradient gels and transferred onto polyvinylidene fluoride membranes (ATTO, Japan). The membranes were incubated with primary Abs at 4 °C overnight and then with alkaline phosphatase-labeled secondary Abs for 1 h at room temperature. The blots were detected by an alkaline phosphatase-conjugated substrate kit (Bio-Rad). For Bcl-2 overexpression and siRNA experiments, a chemiluminescent ECL system was used to

detect the blots. Western blot analyses were performed on data from more than three independent experiments.

Immunofluorescent Staining—PC12 cells on poly-L-lysine-coated glass chamber slides were washed twice with Dulbecco's phosphate-buffered saline containing NGF before the cells were fixed with 4% paraformaldehyde (Wako, Japan) for 30 min and permeabilized with cold 0.2% Triton X-100 for 10 min. After blocking with 2% bovine serum albumin for 1 h, the cells were incubated with primary Abs against Bax, AIF, ERK, or phospho-histone H2AX at 4 °C overnight. The cells were washed and incubated with Alexa 488- or Texas Red-labeled secondary antibodies (Invitrogen) and Hoechst 33342 (Invitrogen) or TUNEL (Roche Diagnostics) at room temperature for 1 h. After washing, the cells were mounted with Prolong gold mounting media (Invitrogen). Fluorescent microscopy was performed using an IX71 microscope (Olympus, Japan), a deconvolution microscope DeltaVision personal DV (Applied Precision), and a Leica confocal microscope TCS-SP5 (Leica Microsystems, Germany). Immunofluorescent staining data were obtained from more than four independent experiments.

Caspase-3/7 Assay—PC12 cells were cultured in 10-cm poly-L-lysine-coated dishes in the differentiation condition. The caspase-3 activity of lysates from PC12 cells treated with ESA was measured with the Apo-ONE homogeneous caspase-3/7 assay kit (Promega) according to the manufacturer's protocol using a fluorescent plate reader (Infinity M, Tecan). Data were obtained from two independent experiments.

DNA Analysis—Genomic DNA was extracted from the cells treated with α-ESA for 30 h using FastPure DNA kit (Takara, Japan), and DNA was analyzed using agarose gel electrophoresis and pulse field gel electrophoresis (CHEF DR-II, Bio-Rad). The conditions for the pulse field gel electrophoresis were as follows: 1% agarose, 6 V/cm, 15 °C, 15 h.

Bcl-2 Transfection—The human *bcl-2* was a kind gift from Y. Tsujimoto (Osaka University, Japan). The *bcl-2* was subcloned into the pcDNA-DEST40 expression vector (Invitrogen). PC12 cells (2×10^6 cells/ml) were transfected with the *bcl-2* by an electroporation method (Amaxa Nucleofector II; Lonza, Switzerland) according to the manufacturer's protocol (program U-029). The same numbers of the transfected cells were seeded to 35-mm dishes in the differentiation condition. Twenty four hours after the transfection, the cells were exposed to α-ESA for an additional 24 h. The cell viability was then measured using the WST-8 reagent, and Western blot analysis was performed to check Bcl-2 protein expression. Blots were detected using ECL plus (GE Healthcare) and Hyperfilm (GE Healthcare) following horseradish peroxidase-labeled secondary Abs.

RNA Interference—The knockdown of PARP-1 was performed in PC12 cells using predesigned ON-TARGET*plus* siRNA SMART pool purchased from Dharmacon. The transfection efficiencies were optimized using siRNA optimization kit (Amaxa). The transfections were performed by the electroporation method (Amaxa, program U029), and the same numbers of the transfected cells were seeded to 35-mm dishes. After 24 h of incubation in the differentiation condition, the cells were exposed to α-ESA or MNNG (500 μM, 15 min) for an additional 24 h. ON-TARGET*plus* nontargeting siRNA pool (300 nM) was used as a control for nonsequence-specific effects. The knockdown of MEK1/2 was performed using predesigned Stealth Select siRNA (1 μM) purchased from Invitrogen. Two mixed primers for each target (MEK1 or MEK2) were used for the experiments. Map2k1-RSS301293 and -RSS301295 are for MEK1. Map2k2-RSS339849 and -RSS339850 are for MEK2 (Invitrogen). Stealth RNA interference negative control was used as a control for nonsequence-specific effects. The cell viability was then measured using the WST-8 reagent, and Western blot analysis was performed to check protein expression. The blots were detected using ECL Plus (GE Healthcare) or an alkaline phosphatase-conjugated substrate kit (Bio-Rad).

Microinjection of AIF Antibody—AIF antibody (100 μg/ml, mouse IgG2b) or MOPC21 (100 μg/ml, isotype control for IgG2b) was microinjected into the differentiated PC12 cells using Stamporation apparatus SU100 (Olympus, Japan) and StampoNeedle (ST-ME330CN-20A, Olympus) (25) in 35-mm poly-L-lysine-coated culture dishes. The microinjected cells were exposed to α-ESA (2 μg/ml) after a 6-h incubation. After 16 h of treatment with α-ESA, the cells were stained with propidium iodide.

Bax Localization—The differentiated PC12 cells were treated with staurosporine (STS, 500 nM) or α-ESA (2 μg/ml). The cells were fixed and stained with Bax and MitoTracker Red CM-H2XRos (1 μM).

Measurements of ROS and Potential—Intracellular ROS and mitochondrial superoxides were measured using H2DCF-DA (10 μM) and MitoSOX Red (5 μM), respectively. Differentiated PC12 cells were incubated with CM-H2DCF-DA or MitoSOX for 1 h or 10 min, respectively. After washing, α-ESA was added to the cells. After 2, 5, and 20 h of incubation, the cells were counted to calculate the percentages of ROS-positive cells from a total of 100 cells. Cells that have fluorescent intensities more than the signal to noise ratio of >5 were determined to be positive. ImageJ (version 1.41) software was used to analyze the intensities of the cells. Mitochondrial membrane potential was measured using JC-1 (5 μM).

Statistical Analysis—All data are expressed as the mean ± S.D. The statistical significance was evaluated by one-way analysis of variance followed by the Dunnett's test to compare the data from multiple groups against a common control group (SigmaPlot). Student's *t* test was used to compare the data from two groups. Statistical significance was determined at $p < 0.05$ (indicated with an *asterisk* in the figures).

RESULTS

α-ESA Induces Apoptosis in Neuronal Cells—The time course illustration of the experiments using α-ESA (Fig. 1*A*) were shown with the morphological and nuclear changes in Fig. 1*B*. In both proliferating (nondifferentiated) and differentiated cells, apoptotic cell death was initiated. PC12 cells were seeded 18 h before the addition of NGF. NGF induced strong ERK1/2 phosphorylation between 7 min and 1 h, resulting in the differentiation and neurite outgrowth. Forty eight hours after the addition of NGF, the phosphorylation of ERK1/2 decreased to the basal level. Then α-ESA (2 μg/ml) was added to the differentiated PC12 cells (Fig. 1*C*). α-ESA induced apoptotic cell death in a dose-dependent manner in neuronal PC12, SH-SY5Y, and NG108-15 cells (Fig. 1*D*). The α-ESA-mediated

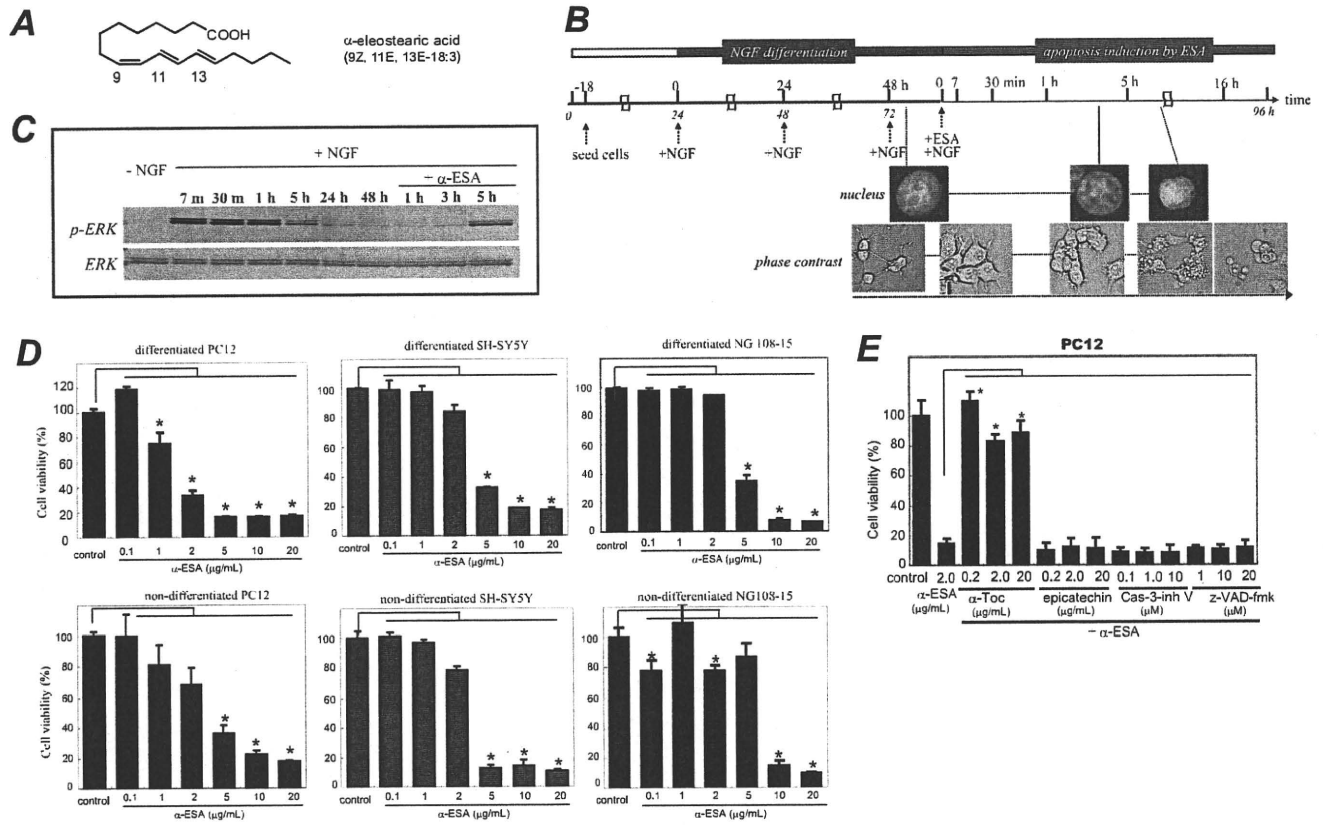

FIGURE 1. **α-ESA induces apoptotic cell death in neuronal cells.** *A*, structure of α-ESA. *B*, time course of α-ESA-mediated cell death in the differentiated PC12 cells. The cells were differentiated by NGF for 48 h and then exposed to α-ESA. *C*, time course of phosphorylation of ERK1/2 during NGF and α-ESA treatment. NGF induced a strong phosphorylation of ERK1/2, and its phosphorylation decreased to the basal level by 48 h. Then the addition of α-ESA induced prolonged and moderate phosphorylation of ERK1/2 again, resulting in the cell death. *D*, α-ESA (2 μg/ml) induced apoptotic cell death in neuronal PC12, SH-SY5Y, and NG108-15 cells. $n = 9$; $p < 0.05$ *versus* control (DMSO alone). *E*, α-ESA-mediated apoptosis was not inhibited by pan-caspase inhibitor Z-VAD-fmk and caspase-3 inhibitor in PC12 cells. α-Toc, but not epicatechin, inhibited the cell death. The values represent the means ± S.D. The viability of α-ESA treated cells was measured by WST-8 reagent 16 h after the treatment. *, $p < 0.05$.

cell death was not inhibited by the pan-caspase inhibitor Z-VAD-fmk and caspase-3 inhibitor V (Z-D(OMe)QM-D(OMe)-fmk) (Fig. 1*E*). Methyl ester of α-ESA did not induce cell death (supplemental Fig. S1).

Effects of MAPK Inhibitors and Antioxidants on α-ESA-mediated Cell Death—A variety of inhibitors was tested to clarify the mechanisms by which α-ESA provoked apoptotic cell death (Fig. 2 and supplemental Fig. S1). The MEK1/2 inhibitor U0126, which inhibits MEK1/2 activity and thereby blocks ERK1/2 phosphorylation, completely abrogated the α-ESA-mediated cell death at a concentration of 5 μM in both nondifferentiated and differentiated cells (Fig. 2*A*). The suppression of phosphorylated ERK1/2 may be important. The cell death was not inhibited by the c-Jun N-terminal kinase (JNK) inhibitor SP600125 and the p38 inhibitor SB203580 (Fig. 2*B*).

Next, the effect of antioxidants on the α-ESA-mediated cell death was examined. Cell death was fully abrogated by α-Toc in neuronal PC12 cells (Fig. 2*C*) but was not inhibited by the green tea antioxidant epicatechin (Fig. 1*E*). Other antioxidants, such as flavonoids (including quercetin and luteolin) and β-carotene, did not reduce the α-ESA-mediated cell death.[3] A trace amount (0.01 μg/ml; equivalent to 23 nM) of α-Toc significantly blocked the cell death induced by 2 μg/ml (equivalent to 7.2 μM) α-ESA (Fig. 2*C*). The inhibitory effects of U0126 and α-Toc on the α-ESA-mediated cell death were also observed in SH-SY5Y and NG108-15 cells (Fig. 2*D*). These results suggest that the α-ESA-mediated cell death is not dependent on neurotropic factors such as NGF, retinoic acid, or dibutyryl-cAMP. Thus, ERK1/2 and α-Toc appear to be a key molecule in the α-ESA-mediated apoptotic cell death.

Transient activation of ERK1/2 occurred when PC12 cells were treated with epidermal growth factor, and sustained activation of ERK1/2 occurred when the cells were treated with NGF (26, 27). After NGF stimulation for a few hours, the sustained ERK1/2 phosphorylation decreased to the basal level in our experiments (Fig. 1*C*). α-ESA was then added to the culture media containing NGF, and the ERK1/2 phosphorylation was investigated at variable intervals in PC12 cells (Fig. 3). Similar experiments were performed in the cells that were pretreated with the MEK1/2 inhibitor U0126 or α-Toc for 30 min. Prolonged ERK1/2 phosphorylation that lasted for at least 16 h was observed in the α-ESA-treated PC12 cells as well as in the camptothecin (CPT)-treated cells. ERK1/2 phosphorylation was observed 2–6 h after the addition of α-ESA and strongly increased by 16 h. U0126 blocked the ERK1/2 phosphorylation

[3] K. Kondo, S. Obitsu, S. Ohta, K. Matsunami, H. Otsuka, and R. Teshima, unpublished data.

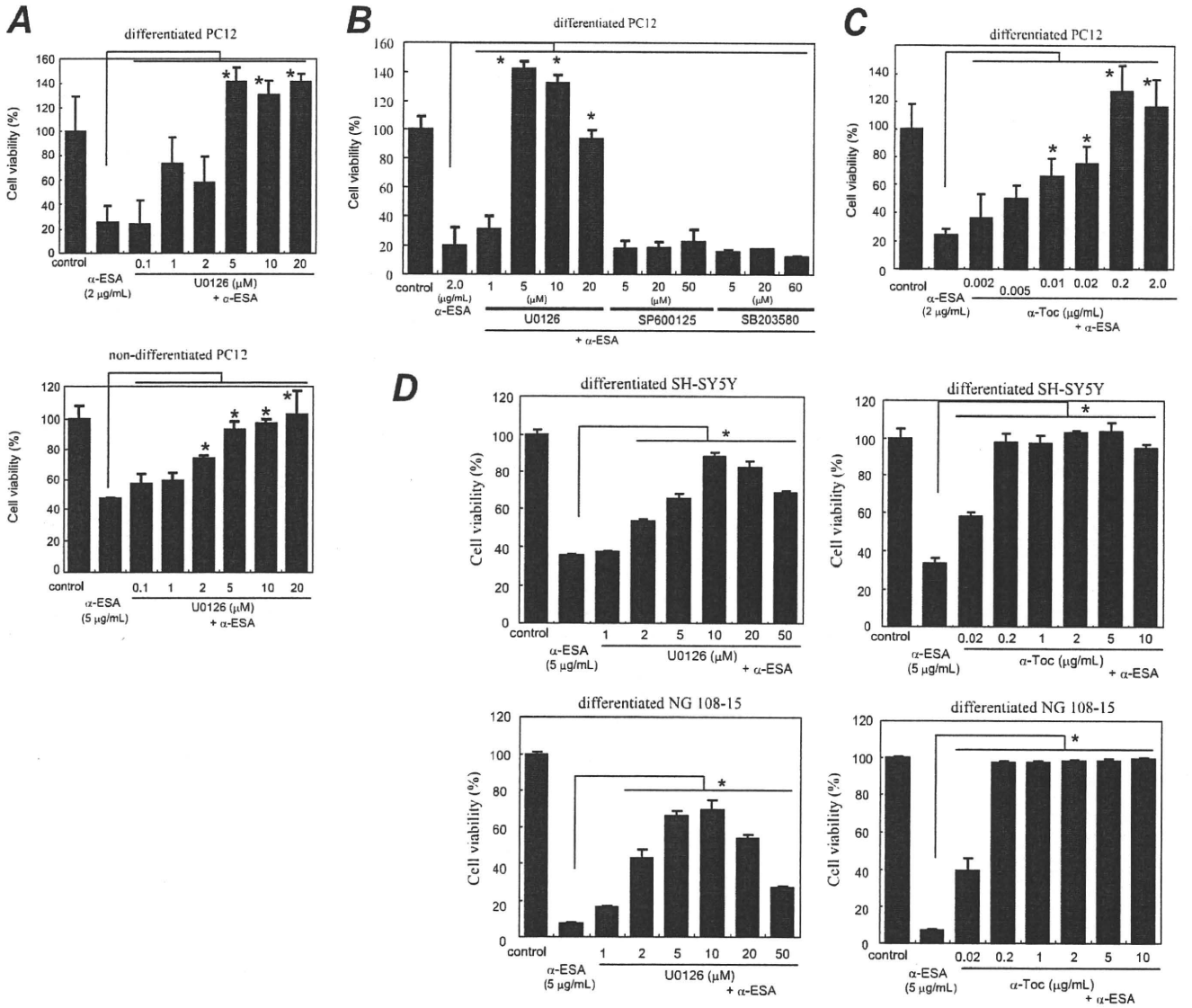

FIGURE 2. **MEK inhibitor and α-tocopherol block α-ESA-mediated cell death.** *A*, MEK inhibitor U0126 prevented α-ESA-mediated cell death in both differentiated and nondifferentiated PC12 cells (5 or 2 μM). $n = 6$; *, $p < 0.05$ *versus* α-ESA alone. *B*, JNK inhibitor SP600125 and p38 inhibitor SB203580 did not block α-ESA-mediated cell death. *C*, α-Toc blocked α-ESA-mediated cell death at lower concentrations (0.01 μg/ml). $n = 6$; *, $p < 0.05$ *versus* α-ESA alone. *D*, in both SH-SY5Y and NG108-15 cells, α-ESA-mediated cell death was blocked by U0126 and α-Toc. The values represent the means ± S.D. The viability of α-ESA treated cells was measured by WST-8 16 h after the treatment.

and thereby prevented the α-ESA-mediated cell death. In contrast, the ERK1/2 phosphorylation was not inhibited by α-Toc, although it completely prevented the cell death (Fig. 3, *A* and *D*). U0126 did not prevent the CPT-initiated apoptosis.[3] These results suggest that the inhibitory mechanism of α-Toc differs from that of U0126.

Next, we examined the activation of caspase-3 during the α-ESA-mediated apoptosis. Caspase-3 was not cleaved to yield an active fragment by α-ESA stimulation over a 16-h time course (Fig. 3*A*). The enzyme activity of caspase-3 was also measured using the fluorescent substrate bis-(*N*-benzyloxycarbonyl-L-aspartyl-L-glutamyl-L-valyl-aspartic acid amide)-rhodamine 110 (Z-DEVD-rhodamine 110). The activity of caspase-3 markedly increased in the CPT-treated cells, whereas no increase in the caspase-3 activity was observed in the α-ESA-treated cells (Fig. 3*B*). CPT was used as a positive control of caspase-3 activation.

ERK1/2 translocation to the nucleus was investigated using confocal microscopy. ERK1/2 migrated to the nucleus 4 h after the induction of apoptotic cell death by α-ESA (Fig. 3*C*). *YZ* planar images confirmed that ERK1/2 was localized in the nucleus. This result was consistent with Western blot analysis data. Actin rearrangement was abrogated in PC12 cells treated with α-ESA. The growth cone of neurite of the cells was significantly suppressed, showing the retardation of pseudopods.

AIF Translocation to the Nucleus and Chromatin Condensation—We next investigated AIF migration upon α-ESA treatment. ERK1/2 was localized in the nucleus when PC12 cells were treated with α-ESA as described above. AIF was initially localized in the mitochondria and migrated to the

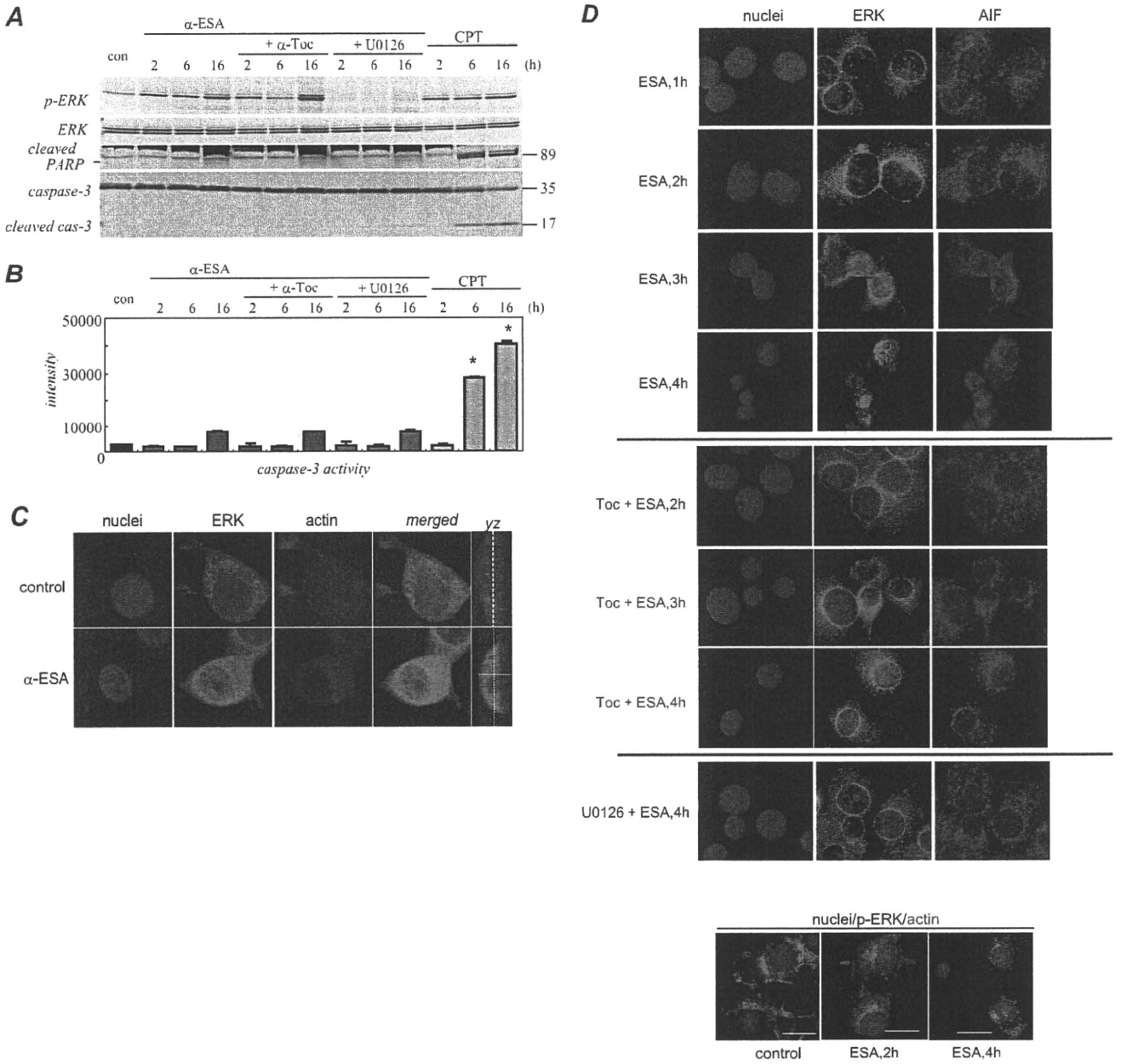

FIGURE 3. **ERK1/2 phosphorylation, PARP-1, and caspase-3 activation induced by α-ESA.** *A,* Western blot samples were prepared from PC12 cells at different time points (2, 6, and 16 h). Western blot analysis was independently repeated three times, and representative data are shown here. ERK1/2 was phosphorylated 2 h or later after α-ESA treatment. U0126 blocked the phosphorylation, whereas α-Toc did not. The cleaved form of PARP-1 (89 kDa) and the active form of caspase-3 (17 kDa) were not detected in α-ESA-treated cells. *con,* control. *B,* caspase-3 enzymatic activity was measured using a fluorescent substrate. The activity remained at the basal level until 6 h after the induction of apoptosis by α-ESA. CPT was used as a positive control of caspase-3 activity. *, $p < 0.05$ *versus* control (DMSO alone). *C,* ERK1/2 migrated to the nucleus upon α-ESA treatment. Images were obtained from samples treated with α-ESA for 4–5 h. Growth cone disappeared, and the actin rearrangements were suppressed. The confocal microscopy images showed that ERK1/2 was localized throughout the nucleus. *D,* treatment of U0126, but not α-Toc, blocked nuclear localization of ERK1/2. The nuclear localization of ERK1/2 and AIF was observed in the α-ESA-mediated cells. Phosphorylated ERK1/2 was observed in the nucleus (*bottom panel*).

nucleus upon α-ESA treatment. At 4 h after the induction of apoptotic cell death, AIF was translocated from the mitochondria to the nucleus, and the number of TUNEL-positive cells was increased. By 7 h after the induction of apoptosis, AIF was mostly localized in the nucleus and DNA compaction occurred (Fig. 4*A*). It was previously reported that when caspase-independent apoptosis was induced, AIF caused the cleavage of DNA into large fragments (~50 kb), which was referred to as stage-I apoptosis (28). Similar DNA cleavage was observed in the α-ESA-treated cells, which was not associated with nucleosomal DNA fragmentation. Pulse field gel electrophoresis revealed the cleavage of DNA into large scale (30–50 kb) fragments in neuronal PC12 cells (Fig. 4*B*). In deconvolution analysis, 30 slices of images were obtained to rebuild three-dimensional images. Data analysis was done using ImageJ software. This result clearly shows AIF localization in the nucleus and the TUNEL-positive nucleus. The subcellular fractions were analyzed by Western blotting. AIF was released from the mito-

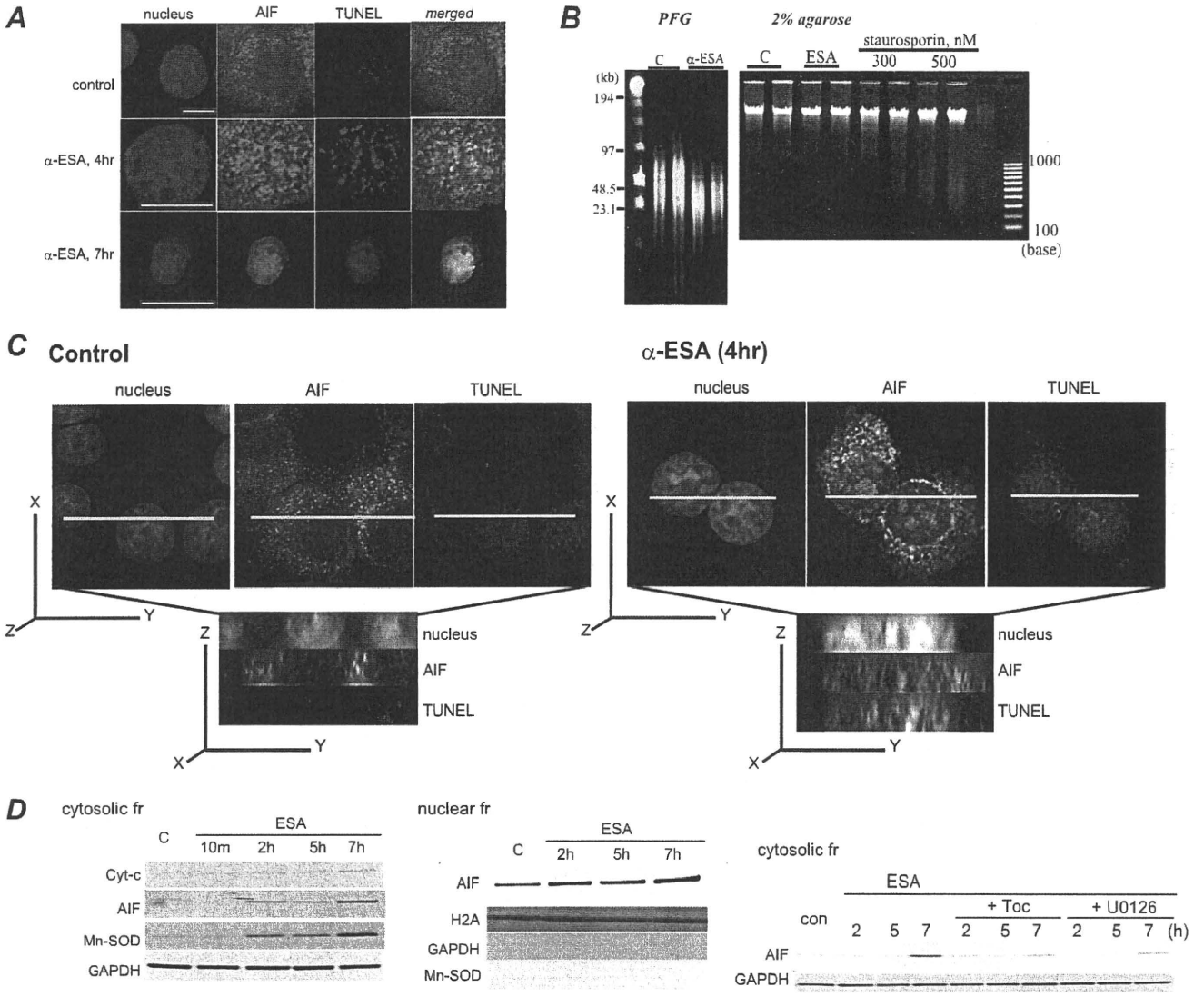

FIGURE 4. **AIF translocation to the nucleus by α-ESA.** *A*, α-ESA induced AIF translocation from the mitochondria to the nucleus. At 4 h after the induction of apoptosis by α-ESA, AIF was translocated to the nucleus (*green*). The nucleus was stained with TUNEL (*red*) and Hoechst (*blue*). *Scale bars* show 10 μm. The TUNEL staining was scattered. By 7 h, the nucleus greatly condensed, and AIF spread throughout the nucleus. The peripheral distribution of chromatin in the α-ESA-treated cell shown was characteristic of AIF-induced stage-I condensation. Images were obtained using the deconvolution microscope. *B*, DNA analysis. Genomic DNA was extracted from PC12 cells that were treated with either DMSO as a control or α-ESA (2 μg/ml) for 30 h. The extracted DNA was analyzed by pulse field gel (*PFG*) electrophoresis. High molecular weight fragments (30–50 kb) were detected on pulse field electrophoresis. Nucleosomal DNA fragmentation was analyzed by 2% agarose gel, showing that α-ESA did not induce nucleosomal DNA degradation. *C*, three-dimensional images of AIF localization in the nucleus. AIF was localized in the whole nucleus, and the nucleus was stained with TUNEL. *D*, subcellular fractionation analysis. The release of AIF and manganese superoxide dismutase (*Mn-SOD*) was observed in the cytosolic fraction (*fr*) of α-ESA-treated cells, resulting in AIF-initiated cell death (*left panel*). The Western blotting of the nuclear fraction revealed AIF localization in the nucleus. There is no contamination of cytosolic and heavy membrane fractions, including mitochondria. α-Toc and U0126 blocked AIF release to the cytosolic fraction (*right panel*). *GAPDH*, glyceraldehyde-3-phosphate dehydrogenase.

chondria into the cytosolic fraction of the α-ESA-treated cells, which was in agreement with the findings of microscopic studies (Fig. 4*A*). In addition, manganese superoxide dismutase was detected in the cytosolic fraction 2–7 h after the induction of the cell death (Fig. 4*D*), suggesting that mitochondrial membrane permeabilization occurred in the α-ESA-treated cells. In addition, the increase in the amount of AIF protein in the nucleus is time-dependent. In this fractionation, there was no contamination from the cytosol or heavy membrane fractions. Finally, the inhibitory effect of α-Toc and U0126 on AIF release was investigated. Both α-Toc and U0126 abrogated AIF release.

PARP-1-independent Cell Death—We next found that the α-ESA-mediated cell death was not abrogated by the PARP-1 inhibitor DPQ at concentrations of up to 100 μM. Moreover, no PAR proteins were detected in Western blot analysis (Fig. 5*A*). This suggests that the α-ESA-mediated apoptotic cell death differs not only from caspase-dependent apoptosis but also from caspase-independent and AIF-mediated apoptosis, which always requires PARP-1 activation, as reported elsewhere (29). To our knowledge, no previous report has described AIF-mediated caspase-independent apoptosis without PARP-1 activation.

DNA damage was also evaluated in the α-ESA-treated cells using anti-phosphorylated histone H2AX (γ-H2AX) Ab. Histone H2AX was phosphorylated in response to DNA damages such as double strand breaks by γ-irradiation. The DNA-alkyl-

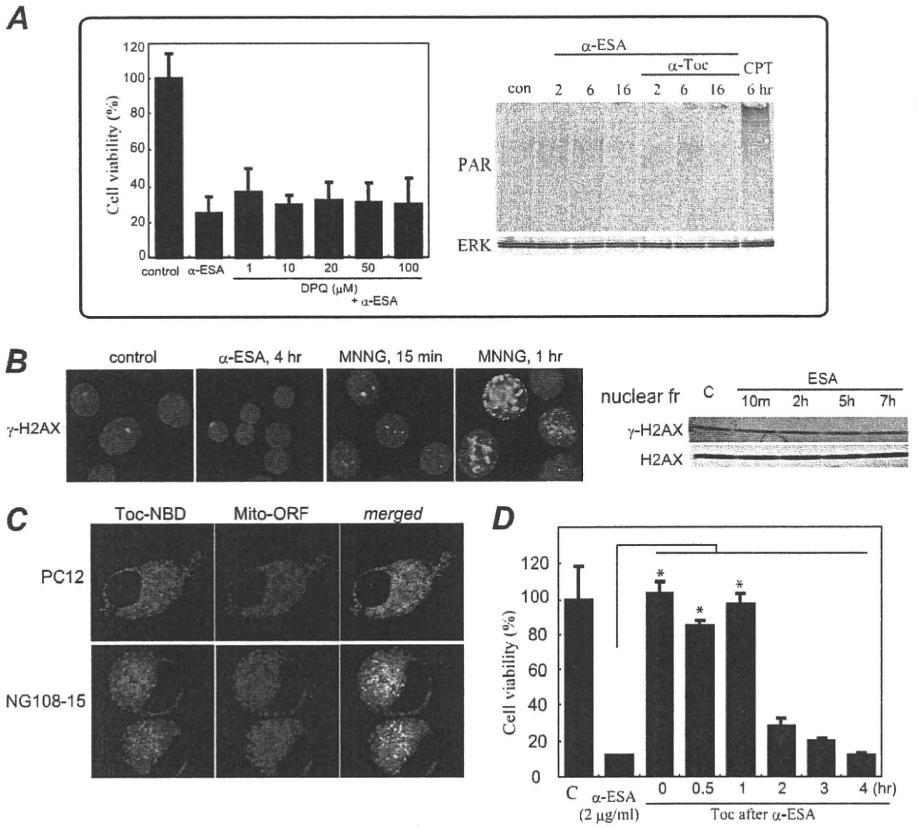

FIGURE 5. *A*, α-ESA-mediated cell death was not inhibited by the established PARP inhibitor DPQ, and PAR proteins were not detected. CPT (40 μM) was used as a positive control for PAR formation. Data were obtained from two independent experiments performed in triplicate (mean ± S.D.). Significance in DPQ-pretreated cells was not observed (*versus* α-ESA alone). *B*, γ-H2AX staining (nuclei in *blue* and γ-H2AX in *green*). Phosphorylation (Ser-139) of histone H2AX (γ-H2AX) was induced by MNNG (500 μM), not by α-ESA (2 μg/ml). γ-H2AX protein levels were not changed in α-ESA-mediated cells. *c*, control. *C*, α-Toc distribution in PC12 and NG108-15 cells was investigated using a confocal microscope. α-Toc is labeled in *green*, and mitochondria are labeled in *red*. The merged images in PC12 and NG108-15 cells show that α-Toc was distributed mostly in the mitochondria. *D*, effect of α-Toc after α-ESA treatment (post-treatment). α-Toc (0.2 μg/ml) was added to the cells at the same time as or after the addition of α-ESA (2 μg/ml). α-Toc blocked cell death 1 h after the addition of α-ESA. Adding α-Toc more than 2 h after α-ESA had no effect. *, $p < 0.05$.

ating agent MNNG induced double strand breaks, whereas α-ESA did not. This indicates that DNA double strand breaks do not arise from the α-ESA-treated cells (Fig. 5*B*).

To clarify the action of α-Toc in these cells, its localization was examined using NBD-labeled α-Toc and orange fluorescent protein-tagged mitochondrial resident protein. In both PC12 and NG108-15 cells, α-Toc mostly migrated to and was localized in the mitochondria (Fig. 5*C*). The localization of α-Toc to the nucleus was not observed in both cell types. The post-treatment with α-Toc 1 h after the addition of α-ESA still blocked the apoptotic cell death (Fig. 5*C*). Recently, ERK1/2 was reported to regulate PARP-1 activation (30, 31). However, PARP-1 itself was not activated in the α-ESA-treated cells.

Microinjection of AIF Antibody—AIF (mouse IgG2b) or MOPC21 (isotype control) antibody was microinjected into the differentiated PC12 cells. The AIF Ab-injected cells blocked the α-ESA-mediated cell death, whereas the MOPC21 Ab-injected cells were killed by α-ESA (Fig. 6*A*). This shows that AIF is a critical factor for the α-ESA-mediated cell death.

Overexpression of Bcl-2—Pro-survival Bcl-2 widely protects apoptosis induced by various stimuli such as camptothecin, etoposide, and staurosporine because Bax/Bak-mediated release of Cyt-c, Smac/Diablo, AIF from mitochondria is blocked by pro-apoptotic Bcl-2 and Bcl-X_L (9, 32, 33). Thus, PC12 cells were transfected with *bcl-2* by the electroporation method (Amaxa Nucleofector II). The amount of Bcl-2 protein in the transfected cells was approximately nine times greater than that in mock-transfected cells according to Western blot analysis. The cell viability was measured using the WST-8 assay reagent for the whole cells. The release of AIF from the mitochondria to the nucleus was suggested to be regulated by Bcl-2 (34). However, the α-ESA-mediated apoptotic cell death was not blocked by Bcl-2 overexpression (Fig. 6*B*). Yu *et al.* (20) reported that Bcl-2 alone was not sufficient to prevent MNNG-treated AIF release and caspase-independent cell death.

RNA Interference of PARP-1 or MEK1/2—α-ESA induced AIF release, resulting in the cell death without PARP-1 activation. The well established PARP-1 inhibitor DPQ did not block the apoptotic cell death. To clarify the involvement of PARP-1 in the α-ESA-mediated cell death, the knockdown experiments for PARP-1 were carried out using siRNA targeted for rat PARP-1. The siRNA-transfected PC12 cells were exposed to α-ESA (2 μg/ml) or MNNG (500 μM) as a positive control in the differentiated condition. The PARP-1 knockdown inhibited the MNNG-treated cell death, whereas the knockdown did not abrogate the α-ESA-mediated cell death (Fig. 6*C*). DPQ treatment of PARP-1 knockdown cells also did not block the cell death (Fig. 6*D*). These results suggest that PARP-1, which is considered to be required for AIF-initiated caspase-independent apoptosis, is not involved in the α-ESA-mediated cell death.

We next investigated whether or not ERK1/2 phosphorylation was critical for the α-ESA-mediated cell death using siRNA targeted for rat MEK1/2. The siRNAs for MEK1 or MEK2 were transfected into PC12 cells, and the cells were exposed to α-ESA (5 μg/ml) in the proliferation condition. The knockdown of either MEK1 or MEK2 effectively blocked the α-ESA-mediated cell death (Fig. 6*E*). Together with the inhibitor (U0126) experiments, these results indicate that ERK1/2 phosphorylation plays an important role in the α-ESA-mediated apoptotic cell death.

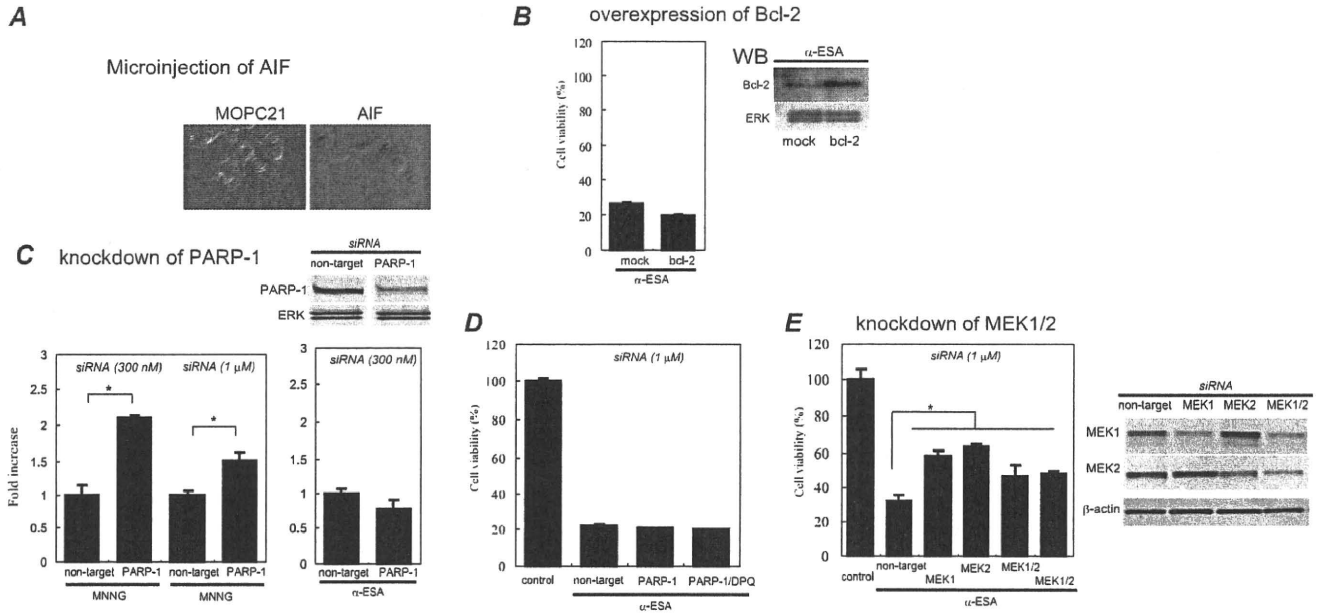

FIGURE 6. **Effect of AIF microinjection, Bcl-2 overexpression, and knockdown of PARP-1 and MEK1/2 on α-ESA-mediated apoptosis.** *A,* microinjection of AIF antibody blocks α-ESA-mediated apoptosis. AIF or MOPC21 (isotype control) antibody (*Ab*) was microinjected into the differentiated PC12 cells using Stamporation apparatus and incubated for 6 h. The cells were exposed to α-ESA (2 μg/ml) for 16 h and stained with propidium iodide. The AIF Ab-microinjected cells blocked α-ESA-mediated cell death, whereas the MOPC21 Ab-microinjected cells did not, stained in *red,* which means the cells were dead. Images were obtained from three independent experiments. All cells in these images were microinjected. *B, bcl-2* was transiently transfected into PC12 cells. After 24 h of incubation, the cells were exposed to α-ESA (2 μg/ml) and incubated for another 16 h. The cell viability was measured for the whole cells. The overexpression of Bcl-2 did not protect PC12 cells from α-ESA-mediated apoptosis ($n = 3$). *WB,* Western blot. *C,* siRNA targeted for rat PARP-1 was transfected into PC12 cells. After 24 h of incubation, the cells were exposed to α-ESA (2 μg/ml) or MNNG (500 μM) and incubated for another 16 h. The cell viability was measured for the whole cells. The knockdown of PARP-1 did not block α-ESA-mediated apoptosis, whereas it prevented MNNG-treated (500 μM, 15 min) cells from the apoptosis. ($n = 3$; *, $p < 0.001$). *D,* combination of PARP-1 knockdown and DPQ treatment (50 μM) had no effect on the block of the apoptosis. *E,* siRNA experiments for rat MEK1 and MEK2 were performed in the proliferation condition. The knockdown of either MEK1 or MEK2 significantly blocked α-ESA-mediated cell death ($n = 6$; *, $p < 0.05$). The knockdown of both MEK1 and MEK2 also inhibited the cell death. The transfection efficiency was ~80% judging from the cells transfected with cDNA encoding green fluorescent protein. The blots for the knockdown samples are shown in the *right panel.* The cell viabilities were measured for the whole cells in overexpression and knockdown experiments.

Involvement of Superoxide Anion Radicals and Mitochondrial Membrane Potential in α-ESA-mediated Cell Death—Involvement of ROS in the α-ESA-mediated apoptotic cell death was next investigated using fluorescent probes, CM-5-(and-6)-chloromethyl-2′,7′-dichlorodihydrofluorescein diacetate for total ROS and BESSo-AM (35, 36) and MitoSOX Red for superoxide anion radicals. Intracellular ROS was observed in the α-ESA-treated cells. The ROS production was blocked by α-Toc pretreatment, whereas epicatechin was not able to inhibit ROS production and the apoptotic cell death (Fig. 7*A*). Superoxide anion radicals were produced shortly before the α-ESA-mediated plasma membrane blebbing started (Fig. 7*B*). Some BESSo-positive cells showed normal morphology, and some of the cells started plasma membrane blebbing. The production of superoxide anion radicals was time-dependent. The strongest intensity was observed 5 h after α-ESA treatment. Superoxide anion radicals produced by α-ESA are probably a small quantity because a trace amount of α-Toc (0.01 μg/ml) localized mostly in the mitochondria abrogated the apoptotic cell death. It appears that the α-ESA-mediated cell death is different from that induced by a high concentration of 1-methyl-4-phenylpyridine or 3-nitropropionic acid (>1 mM), which can produce a large amount of ROS and activate caspase. Superoxide production was also measured using MitoSOX Red to detect superoxides in the mitochondria. Superoxide was produced in the α-ESA-treated cells, whereas the cells pretreated with α-Toc scavenged superoxides (Fig. 7*C*). U0126 almost blocked superoxides.

Mitochondrial membrane potential ($\Delta\Phi_m$) was next examined using JC-1 staining. An uncoupler, carbonyl cyanide *p*-chlorophenylhydrazone, in the mitochondria-electron transport chain immediately abrogated the potential. In contrast, the mitochondrial membrane potential gradually decreased over 5 h in the α-ESA-treated cells (Fig. 7*D*). These results suggest that α-ESA initiates a small amount of superoxide anion radicals, thereby inducing the reduction in the mitochondrial membrane potential, which results in the cell death associated with the plasma membrane blebbing.

Bax Localization of α-ESA-mediated Cells—In the STS-treated cells, Bax started to translocate into the mitochondria at 4 h. However, Bax migration to the mitochondria was not observed in the α-ESA-mediated cells (Fig. 8). These results suggest that Bax-induced channel formation in the mitochondrial outer membrane is not involved in the α-ESA-mediated cell death. The data that Cyt-c was not released from the mitochondria into the cytosol before AIF (Fig. 4*D*) support this result.

Putative Cell Death Mechanism Induced by α-ESA—When cells were treated with STS or actinomycin D in the presence of Z-VAD-fmk, caspase activation was blocked. However, Bax and Bak are localized in the mitochondria, resulting in the release of Cyt-c, AIF, and other mitochondrial proteins such as Smac/

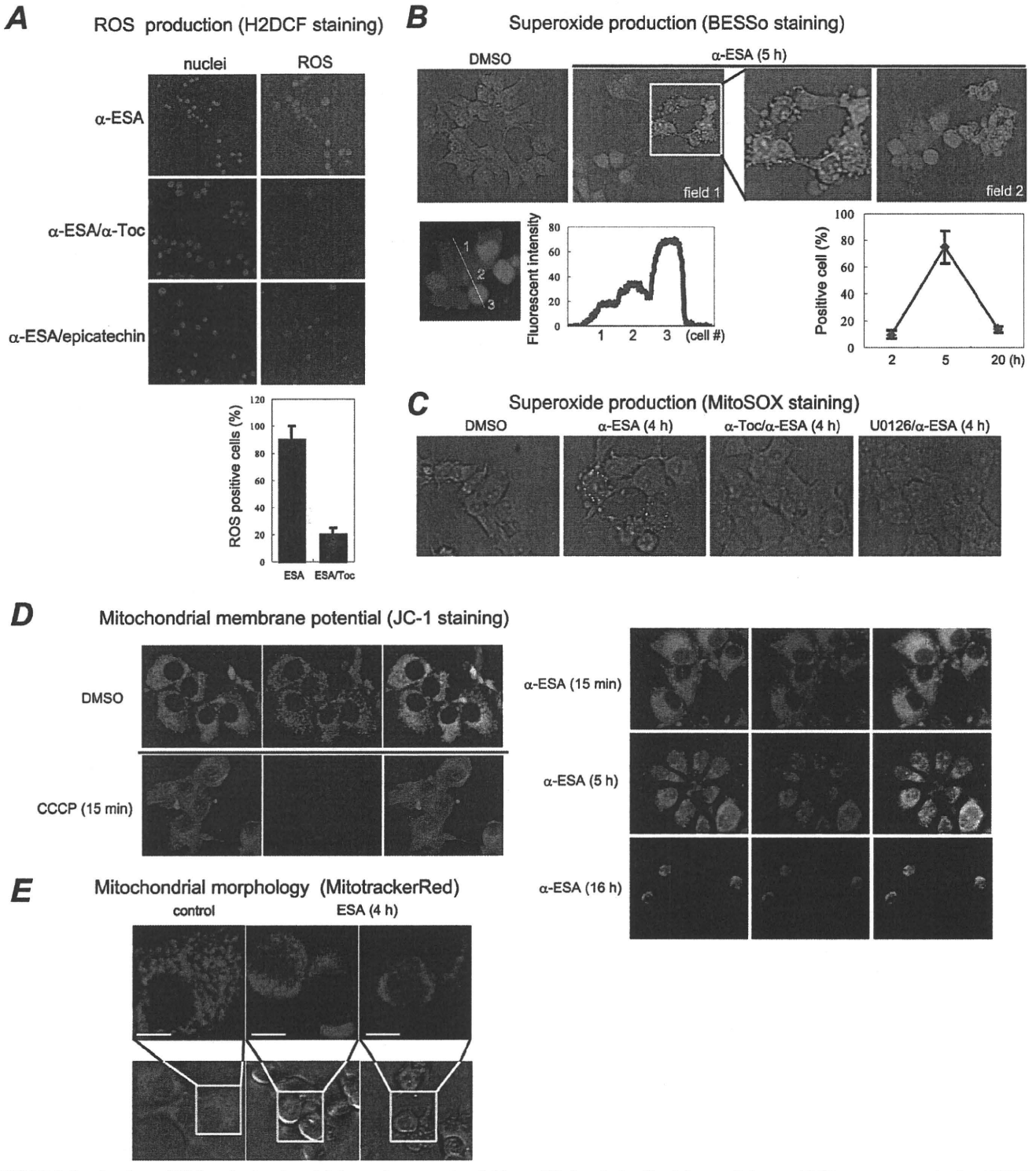

FIGURE 7. **Production of ROS and mitochondrial membrane potential in α-ESA-treated cells.** *A*, intracellular total ROS was measured using H2DCF fluorescent probe. α-ESA initiated ROS, which was blocked by α-Toc (2 μg/ml) but not epicatechin (20 μM). The numbers of ROS-positive cells were counted in the α-ESA-treated cells (12 h) with or without α-Toc. *B*, production of superoxide anion radicals ($O_2^{\cdot-}$) was measured using BESSo fluorescent probe, specific for $O_2^{\cdot-}$. Fluorescent intensities were analyzed by ImageJ software. The cell numbers 2 and 3 that have fluorescent intensities more than the signal to noise ratio of >5 were positive. $O_2^{\cdot-}$ production was observed 5 h after the addition of α-ESA (*bottom right*). Membrane blebbing was observed immediately after superoxide production. *C*, $O_2^{\cdot-}$ was measure by MitoSOX Red indicator. $O_2^{\cdot-}$ was produced in α-ESA-treated cells. α-Toc (2 μg/ml) inhibited the $O_2^{\cdot-}$ production. U0126 (5 μM) almost blocked the $O_2^{\cdot-}$ production. *D*, mitochondrial membrane potential was measured using JC-1. Carbonyl cyanide *p*-chlorophenylhydrazone (*CCCP*) (50 μM) immediately shut down the potential. α-ESA gradually reduced the potential. *E*, mitochondrial morphology during α-ESA-mediated cell death process. Fragmented and condensed mitochondria were observed in the α-ESA-treated cells. *Scale bars* show 8 μm.